MAGNETIC RESONANCE IMAGING AND SPECTROSCOPY BIOMARKERS IN HEREDITARY MUSCLE DISEASES

by
Doris G. Leung

A dissertation submitted to Johns Hopkins University in conformity with the requirements for the degree of Doctor of Philosophy

Baltimore, Maryland

October, 2016

Abstract

Statement of problem: Clinical research in hereditary muscle disease is limited by the absence of quantitative and objective biomarkers and outcome measures that track disease severity. A growing body of literature supports the use of magnetic resonance imaging (MRI) as a potential biomarker of disease in skeletal muscle. The work presented seeks to examine the viability of magnetic resonance-based biomarkers in muscular dystrophy.

Methods: We conducted a systematic review of publications reporting MRI findings in skeletal muscle in muscular dystrophy and congenital myopathy populations. We subsequently performed an observational study of whole-body MRI in people with type 1 facioscapulohumeral muscular dystrophy (FSHD) to characterize the frequency and severity of muscle involvement in this population. We then used a multivoxel magnetic resonance spectroscopy (MRS) protocol to obtain metabolite concentration profiles of skeletal muscle in people with FSHD. These profiles were compared to those of healthy volunteers. The associations between MRI/MRS measurements and clinical strength and function were examined using linear regression models.

Results: A systematic review of the literature on MRI in hereditary myopathies showed widely variable methods of analysis and reporting. However, distinctive patterns of muscle involvement can be identified in some diseases. Whole-body MRI was used to characterize muscle involvement and sparing in FSHD. MRS further identified differences in muscle metabolite concentrations in people with FSHD compared to healthy controls. Both MRI and MRS measurements showed a significant association with strength in specific muscle groups.

Conclusions: MRI and MRS can be used to identify patterns of disease and assess disease severity in the muscular dystrophies. Longitudinal studies are needed to develop imaging techniques as biomarkers for use in clinical trials and observational studies.

Thesis committee members:

Kathryn R. Wagner, M.D., Ph.D.

Edgar R. Miller, III, M.D., Ph.D.

Naresh M. Punjabi, M.D., Ph.D.

Martin A. Lindquist, Ph.D.

Michael A. Jacobs, Ph.D.

Alternate thesis committee members:

Allan C. Gelber, M.D., M.P.H., Ph.D.

Brian S. Caffo, Ph.D.

Acknowledgements

Funding for the research presented in this dissertation was provided by the following grants:

- The Johns Hopkins Clinical Research Scholars Program: KL2TR001077
- The National Institutes of Neurological Disorders and Stroke Mentored Patient-Oriented Research Career Development Award: 5 K23 NS091379
- The American Academy of Neurology Foundation Clinical Research Training Fellowship
- The FSH Society Irene Lai research grant: FSHS-82011-02
- The Senator Paul D. Wellstone Muscular Dystrophy Cooperative Research Center for FSHD: 5U54HD060848-02

I offer my deepest thanks to Dr. Kathryn Wagner for her continued support for my research over the past six years. Her dedicated mentorship is a stellar example for educators and scientists in our field.

I also thank the members of my thesis committee for their thoughtful comments and encouragement. Their contribution to this work and my development as a scientist cannot be overstated.

This work could not have been completed without the collaboration and commitment of the following members of the Johns Hopkins Department of Radiology and Radiological Science: Drs. Michael Jacobs, Peter Barker, John Carrino, Li Pan, and Xin Wang. I also wish to recognize the contribution of Hugh Wall, Cynthia Maranto, and Cynthia Schultz, the technicians from the Division of MR Research who have been present for every single scan.

Finally, I acknowledge the generous contribution of the volunteers who participated in this study.

Table of Contents

List of Tables

List of Figures

Introduction

The muscular dystrophies

The muscular dystrophies comprise a broad class of hereditary progressive muscle disorders. All of the muscular dystrophies are rare diseases (the most common form, Duchenne muscular dystrophy, occurs in 1:5,000 male births).[1] However, the progressive weakness and multi-systemic medical complications that accompany these illnesses lead to a disproportionately high burden of disease in affected patients. Health care utilization data further indicate that there is a considerable cost of care for these chronic illnesses.[2,3]

Mutations in any of the numerous genes involved in the structure and function of muscle can cause muscular dystrophy, and the numbers of disease-causing mutations in humans continue to grow with the increasing use of genetic testing.[4] Many muscular dystrophies are caused by mutations in genes that encode key structural proteins in muscle. One of these proteins is dystrophin, a large protein that links actin (a component of the muscle cytoskeleton) and the dystroglycan complex located in the sarcolemma (the muscle cell membrane). Mutations in dystrophin cause Duchenne and Becker muscular dystrophy, which are among the best characterized muscular dystrophies. Defects in genes that engage in muscle membrane repair (dysferlin), nuclear envelope stability (lamin A/C), intracellular signaling (calpain), and attachment of muscle to the extracellular matrix (laminin alpha 2) can also cause muscular dystrophy (Table 1).[5]

Muscular dystrophies can also be caused by mechanisms other than single-gene, loss-of-function mutations. The myotonic dystrophies, for example, are repeat expansion diseases. In this class of disorders, excessive numbers of repeated short sequences of DNA produce mRNA expansions that bind and sequester proteins in the nucleus. These proteins are required for the correct splicing of multiple genes, and their

sequestration affects multiple systems (including the gastrointestinal, cardiac, endocrine, and ocular systems) in addition to muscle.[6,7] Facioscapulohumeral muscular dystrophy (FSHD) is another example of a genetic disease that is not caused by a loss-of-function gene mutation. Although the pathological mechanisms that cause FSHD are incompletely understood, it is now recognized as a disorder of epigenetic function in which hypomethylation of DNA in the long arm of chromosome 4 leads to gain-of-function effects through the unsuppressed expression of normally dormant genes.[8]

The muscular dystrophies are phenotypically diverse. The spectrum of skeletal muscle disease can range from clinically undetectable muscle involvement to near-complete paralysis. The distribution of muscle weakness can also vary within the different types of muscular dystrophy. For instance, different mutations in the dysferlin gene can produce distal-predominant weakness (called Miyoshi myopathy) or a more typical limb-girdle phenotype characterized by proximal muscle weakness.[9] At the same time, the muscular dystrophies have considerable clinical overlap, as mutations in different genes can produce similar patterns of weakness (Figure 1).[4]

Biomarkers in hereditary muscle disease

Over the past decade, several potential therapeutic interventions for muscular dystrophy have been developed and are currently being evaluated in clinical trials. Trials in muscular dystrophy rely heavily on measured strength and timed function tests as primary outcome measures. Although these measures are reflective of the disease state, our early experience in conducting clinical trials in muscular dystrophy suggests that better biomarkers are needed.[10,11] Widely-used functional outcome measures, like the 6-minute walk test, cannot be applied to non-ambulatory subjects, which may exclude potential research participants and limit the generalizability of study results. The validity of these functional tests is also dependent on the cooperation of research participants,

and levels of cooperation can vary considerably between repeated measures. Several clinical trials have shown that the variability of the 6-minute walk test in Duchenne muscular dystrophy patients is larger than expected, which has significantly impacted sample size and power calculations for these trials.[12]

Alternative outcome measures for muscular dystrophy include biomarkers from serum and muscle tissue, but these have limitations as well. Creatine kinase, a biomarker of muscle degeneration, is not uniformly abnormal in muscular dystrophy and can be influenced by non-disease factors such as exercise and muscle mass.[13] Although it is currently the gold standard for ascertaining muscle pathology, skeletal muscle biopsy carries significant practical limitations; these procedures are invasive and provide only localized information on diseases that can be heterogeneous within the same patient or even within a single muscle.

MRI in the study of muscle disease

Multiple investigators have recognized magnetic resonance imaging (MRI) as a potential biomarker for muscle disease.[14,15] The non-invasiveness and excellent safety profile of MR technology are highly advantageous when repeated measurements are required, and MRI scans can be performed in both ambulatory and non-ambulatory subjects. Furthermore, MRI is highly sensitive in detecting muscle inflammation and fatty infiltration, which are prominent pathological features of many muscle diseases. MRI is already becoming a standard practice in the diagnosis and management of inflammatory myopathies, and some studies have suggested a role for MRI in the diagnosis of hereditary myopathies as well.[16] MRI may hold even greater promise as a research tool than as a diagnostic tool, as it can fulfill the need for objective outcome measures that are sensitive to disease-related changes in a highly variable population.

The majority of MRI protocols that have been used to study muscle include T1-weighted imaging. T1 relaxation times are based on the speed at which protons realign with a longitudinal magnetic field after being pushed into a transverse plane by a radiofrequency pulse. As protons in fat realign more quickly than protons in water, T1-weighted images offer sharp contrast between fat and water. This not only allows muscles (with their high water content) to be sharply delineated in relation to the surrounding fat, but it also allows the observation of muscle replacement by fat as disease progresses. The most commonly used methods of describing the fat infiltration are variations on a semi-quantitative scale initially described by Murphy et al.[17] Semi-quantitative scales assign higher scores to muscles with greater levels of fat replacement based on visual inspection of anatomic images. It can be performed relatively quickly since it requires no specialized post-processing procedures and has been used to characterize patterns of muscle involvement and sparing in multiple types of muscular dystrophy.[18]

T2-weighted imaging is also routinely used in the evaluation of muscle disease. With T2-weighted sequences, the signal intensity of each voxel is based on the T2 relaxation time, or the speed at which protons realign in the transverse plane after a radiofrequency pulse. Variants of T2-weighted sequences (such as short tau inversion recovery and fluid attenuated inversion recovery) are “fluid-sensitive,” as the long T2 relaxation time of free water causes it to appear bright on these sequences. This quality is useful in identifying edema or edema-like changes that signify the entry of free water into tissues; these findings are considered to be acute changes associated with myopathy.[19] In studies of myositis, the presence of edema on MRI corresponds to inflammatory infiltrates that signify active disease.[20] Similar inflammatory infiltration has also been observed in some muscular dystrophies.[21] Studies in Duchenne muscular

dystrophy have further determined that the T2 relaxation time is elevated in muscular dystrophy and increases with disease severity.[22]

The overall goal of this work is to review the literature on MRI in the characterization of hereditary muscle diseases and to evaluate potential new methods of using magnetic resonance-based techniques in the study of skeletal muscle. We begin with a systematic review of the literature that identifies specific patterns of fat infiltration in different hereditary muscle diseases. This is followed by a study of whole-body MRI in individuals with FSHD and a comparison of metabolic profiles derived from magnetic resonance spectroscopy in people with FSHD compared to unaffected controls. The associations between imaging-based measurements and muscle strength and function are also explored.

References

1. Mah JK, Korngut L, Dykeman J, Day L, Pringsheim T, Jette N. A systematic review and meta-analysis on the epidemiology of Duchenne and Becker muscular dystrophy. Neuromuscular disorders : NMD 2014;24:482-91.

2. Landfeldt E, Lindgren P, Bell CF, et al. The burden of Duchenne muscular dystrophy: an international, cross-sectional study. Neurology 2014;83:529-36.

3. Teoh LJ, Geelhoed EA, Bayley K, Leonard H, Laing NG. Health care utilization and costs for children and adults with duchenne muscular dystrophy. Muscle & nerve 2016;53:877-84.

4. Thompson R, Straub V. Limb-girdle muscular dystrophies - international collaborations for translational research. Nature reviews Neurology 2016;12:294-309.

5. Bhatnagar S, Kumar A. Therapeutic targeting of signaling pathways in muscular dystrophy. J Mol Med (Berl) 2010;88:155-66.

6. Wang ET, Cody NA, Jog S, et al. Transcriptome-wide regulation of pre-mRNA splicing and mRNA localization by muscleblind proteins. Cell 2012;150:710-24.

7. Freyermuth F, Rau F, Kokunai Y, et al. Splicing misregulation of SCN5A contributes to cardiac-conduction delay and heart arrhythmia in myotonic dystrophy. Nat Commun 2016;7:11067.

8. Calandra P, Cascino I, Lemmers RJ, et al. Allele-specific DNA hypomethylation characterises FSHD1 and FSHD2. Journal of medical genetics 2016;53:348-55.

9. Paradas C, Llauger J, Diaz-Manera J, et al. Redefining dysferlinopathy phenotypes based on clinical findings and muscle imaging studies. Neurology 2010;75:316-23.

10. Tawil R, Padberg GW, Shaw DW, van der Maarel SM, Tapscott SJ, Participants FW. Clinical trial preparedness in facioscapulohumeral muscular dystrophy: Clinical,

tissue, and imaging outcome measures 29-30 May 2015, Rochester, New York. Neuromuscular disorders : NMD 2016;26:181-6.

11. Statland JM, McDermott MP, Heatwole C, et al. Reevaluating measures of disease progression in facioscapulohumeral muscular dystrophy. Neuromuscular disorders : NMD 2013;23:306-12.

12. Bushby K, Finkel R, Wong B, et al. Ataluren treatment of patients with nonsense mutation dystrophinopathy. Muscle & nerve 2014;50:477-87.

13. Zhang Y, Huang JJ, Wang ZQ, Wang N, Wu ZY. Value of muscle enzyme measurement in evaluating different neuromuscular diseases. Clinica chimica acta; international journal of clinical chemistry 2012;413:520-4.

14. Mercuri E, Pichiecchio A, Allsop J, Messina S, Pane M, Muntoni F. Muscle MRI in inherited neuromuscular disorders: past, present, and future. Journal of magnetic resonance imaging : JMRI 2007;25:433-40.

15. Wattjes MP, Kley RA, Fischer D. Neuromuscular imaging in inherited muscle diseases. European radiology 2010;20:2447-60.

16. Straub V, Carlier PG, Mercuri E. TREAT-NMD workshop: pattern recognition in genetic muscle diseases using muscle MRI: 25-26 February 2011, Rome, Italy. Neuromuscular disorders : NMD 2012;22 Suppl 2:S42-53.

17. Murphy WA, Totty WG, Carroll JE. MRI of normal and pathologic skeletal muscle. AJR American journal of roentgenology 1986;146:565-74.

18. Hollingsworth KG, de Sousa PL, Straub V, Carlier PG. Towards harmonization of protocols for MRI outcome measures in skeletal muscle studies: consensus recommendations from two TREAT-NMD NMR workshops, 2 May 2010, Stockholm, Sweden, 1-2 October 2009, Paris, France. Neuromuscular disorders : NMD 2012;22 Suppl 2:S54-67.

19. Yao L, Yip AL, Shrader JA, et al. Magnetic resonance measurement of muscle T2, fat-corrected T2 and fat fraction in the assessment of idiopathic inflammatory myopathies. Rheumatology (Oxford, England) 2016;55:441-9.

20. Del Grande F, Carrino JA, Del Grande M, Mammen AL, Christopher Stine L. Magnetic resonance imaging of inflammatory myopathies. Topics in magnetic resonance imaging : TMRI 2011;22:39-43.

21. Tasca G, Pescatori M, Monforte M, et al. Different molecular signatures in magnetic resonance imaging-staged facioscapulohumeral muscular dystrophy muscles. PloS one 2012;7:e38779.

22. Willcocks RJ, Rooney WD, Triplett WT, et al. Multicenter prospective longitudinal study of magnetic resonance biomarkers in a large duchenne muscular dystrophy cohort. Annals of neurology 2016;79:535-47.

Table 1: Genes known to produce hereditary myopathy

Localization	Gene	Protein	Phenotype	Function/pathway
Endoplasmic reticulum	B3GALNT2	B1,3-N-acetylgalactosaminyltransferase 2	Congenital muscular dystrophy	Glycosylation
	GTDC2	Glycosyltransferase-like domain-containing protein 2	Congenital muscular dystrophy	Glycosylation
	SGK196	Protein kinase-like protein SGK196	Congenital muscular dystrophy	Glycosylation
	POMT1	Protein-O-mannosyl transferase 1	LGMD2K	Glycosylation
	POMT2	Protein-O-mannosyl transferase 2	LGMD2N	Glycosylation
	TRAPPC11	Transport protein particle complex subunit 11	LGMD2S	Vesicular/molecular trafficking
	ISPD	Isoprenoid synthase domain	LGMD2U	Glycosylation
Extracellular matrix	COL6	Collagen VI	Bethlem/Ullrich	Basement membrane linkage
	LAMA2	Laminin a2	Congenital muscular dystrophy	Basement membrane linkage
Golgi complex	B3GNT1	B1,3-N-acetylglucosaminyltransferase 1	Congenital muscular dystrophy	Glycosylation
	LARGE	Acetylglucosaminyltransferase-like protein	Congenital muscular dystrophy	Glycosylation
	TMEM5	Transmembrane protein 5	Congenital muscular dystrophy	Glycosylation
	GNE	Glucosamine (UDP-N-Acetyl)-2-Epimerase/N-acetylmannosamine kinase	Distal myopathy	Cell migration, adhesion, signaling
	FKRP	Fukutin related protein	LGMD2I	Glycosylation
	FKTN	Fukutin	LGMD2M	Glycosylation
	POMGnT1	Protein-O-linked mannose B1,2 N-acetylglucosaminyl transferase	LGMD2O	Glycosylation
Lysosomes	GAA	Alpha-1,4 glucosidase	LGMD2V, Pompe	Glycogen storage
Nuclear	MATR3	Matrin 3	Distal myopathy	RNA stabilization
	VCP	Valosin-containing protein	Distal myopathy	Ubiquitin/ proteasome
	EMD	Emerin	EDMD	Nuclear envelope
	SYNE1	Nesprin 1	EDMD	Nuclear membrane stabilization
	SYNE2	Nesprin 2	EDMD	Nuclear membrane stabilization

	LMNA	Lamin A/C	LGMD1B	Nuclear envelope
	TNPO3	Transportin 3	LGMD1F	Nuclear transport
	HNRNPDL	Heterogeneous nuclear ribonucleoprotein D-like protein	LGMD1G	Nuclear transport
	CNBP	CCHC-type zinc finger nucleic acid binding protein	Myotonic dystrophy	RNA splicing
	DMPK	Dystrophia myotonica protein kinase	Myotonic dystrophy	RNA splicing
	PABPN1	Polyadenylate-binding protein nuclear 1	OPMD	RNA regulation
Nuclear/ sarcoplasm	TIA1	TIA-1 Cytotoxic granule-associated RNA binding protein	Distal myopathy	Glycosylation
Sarcolemma	ITGA7	Integrin alpha-7	Congenital muscular dystrophy	Basement membrane linkage
	MEGF10	Multiple EGF like domains 10	Congenital myopathy	Skeletal muscle development
	DMD	Dystrophin	Duchenne/ Becker	Sarcomere, sarcolemma linkage
	CAV3	Caveolin 3	LGMD1C	Membrane stabilization; cell signaling/trafficking
	DYSF	Dysferlin	LGMD2B, distal myopathy	Sarcolemmal repair
	SGCG	Sarcoglycan gamma	LGMD2C	Dystroglycan stabilization
	SGCA	Sarcoglycan alpha	LGMD2D	Dystroglycan stabilization
	SGCB	Sarcoglycan beta	LGMD2E	Dystroglycan stabilization
	SGCD	Sarcoglycan delta	LGMD2F	Dystroglycan stabilization
	ANO5	Anoctamin 5	LGMD2L, distal myopathy	Unknown
	DAG1	Dystroglycan	LGMD2P	Basement membrane linkage
	POPDC1	Popeye Domain-Containing Protein 1	LGMD2X	Cell signaling/trafficking
	SCN4A	Sodium voltage-gated channel alpha subunit 4	Non-dystrophic myotonia	Ion channel
	KCNJ2	Potassium voltage-gated channel subfamily J member 2	Non-dystrophic myotonia	Ion channel
	KCNJ18	Potassium voltage-gated channel subfamily J member 18	Non-dystrophic myotonia	Ion channel
	KCNE3	Potassium voltage-gated channel subfamily E regulatory subunit 3	Non-dystrophic myotonia	Ion channel
Sarcomere	MTM1	Myotubularin 1	Congenital myopathy	Membrane formation/trafficking
	TNNT1	Troponin T type 1	Congenital myopathy	Muscle contraction

	CLF2	Cofilin 2	Congenital myopathy	Muscle contraction
	LMOD3	Leiomodin 3	Congenital myopathy	Muscle contraction
	MYH7	Myosin heavy chain 7	Distal myopathy, hyaline body	Muscle contraction
	BAG3	BLC2-associated athanogene 3	Distal myopathy, myofibrillar	Z-disc
	FLNC	Filamin C	Distal myopathy, myofibrillar	Sarcomere, cytoskeletal architecture
	NEB	Nebulin	Distal myopathy, nemaline, myofibrillar	Muscle contraction
	ZASP	Lim domain-binding 3	Distal myopathy, nemaline, myofibrillar	Z-disc
	TTID	Myotilin	LGMD1A, myofibrillar	Z-disc
	DNAJB6	Heat shock protein 40	LGMD1D	Z-disc
	DES	Desmin	LGMD1E, LGMD2R, distal myopathy	Sarcomere, sarcolemma linkage
	TCAP	Telethonin	LGMD2G, distal myopathy	Z-disc
	TTN	Titin	LGMD2J, distal myopathy	Sarcomere structure
	PLEC1	Plectin	LGMD2Q	Sarcomere, sarcolemma linkage
	LIMS2	Lim and senescent cell antigen-like domains 2	LGMD2W	Cell signaling
	TPM2	Beta-tropomyosin 2	Myofibrillar	Muscle contraction
	TPM3	Gamma-tropomyosin 3	Myofibrillar	Muscle contraction
	ACTA1	Alpha-actin	Nemaline, myofibrillar	Muscle contraction
	CRYAB	aβ-crystallin	Nemaline, myofibrillar	Sarcomere, cytoskeletal architecture
	FHL1	Four-and-a-half-LIM protein 1	X-linked EDMD, reducing body, myofibrillar	Skeletal muscle development
Sarcoplasm	CAPN3	Calpain	LGMD2A	Cytoskeletal repair
	TRIM32	Tripartite motif containing 32	LGMD2H	Ubiquitin/ proteasome
	GMPPB	Mannose-1-phosphate guanyltransferase beta	LGMD2T	Glycosylation
Triad	RYR1	Ryanodine receptor	Congenital myopathy	Ion channel
	DNM2	Dynamin 2	Congenital myopathy	Membrane formation/trafficking
	BIN1	Bridging integrator 1	Congenital	Membrane

			myopathy	remodeling
	KBTBD13	Kelch repeat and BTB domain containing 13	Congenital myopathy	Unknown
	KLHL40	Kelch-like family member 40	Congenital myopathy	Skeletal muscle development
	KLHL41	Kelch-like family member 41	Congenital myopathy	Skeletal muscle development
	SPEG	SPEG complex locus	Congenital myopathy	Skeletal muscle development
	SEPN1	Selenoprotein N	Rigid spine, myofibrillar, multiminicore	Skeletal muscle development
Triad/ perinuclear	CCDC78	Coiled-coil domain-containing protein 78	Congenital myopathy	Nuclear positioning, microtubule function
T-tubule	CLCN1	Chloride voltage-gated channel 1	Non-dystrophic myotonia	Ion channel
	CACNA1S	Calcium voltage-gated channel subunit alpha 1S	Non-dystrophic myotonia	Ion channel

Figure 1: Overlapping phenotypes in genes that produce limb-girdle muscular dystrophy, distal myopathy, and congenital muscular dystrophy

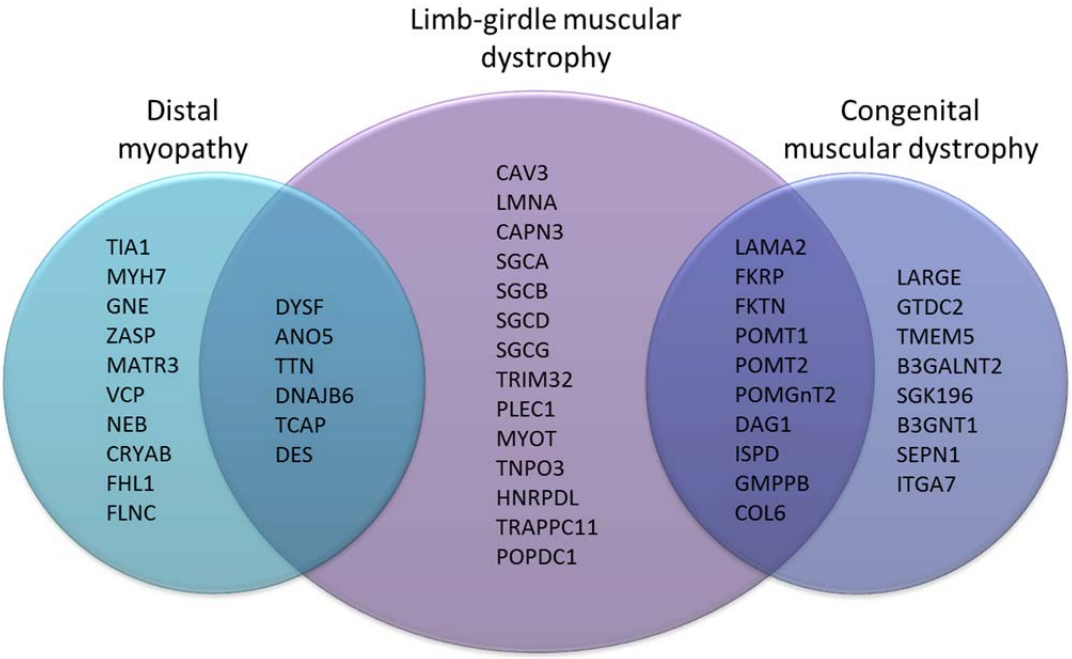

Chapter 1: MRI patterns of muscle involvement in genetic muscle diseases: A systematic review

Abstract

Background: A growing body of literature supports the use of MRI as a potential biomarker for disease progression in the hereditary myopathies.

Objective: To systematically evaluate patterns of fat infiltration reported in MRI studies of muscular dystrophy and congenital myopathy.

Methods: Searches were performed using MEDLINE, EMBASE, and grey literature databases. Studies that described patterns of fat infiltration of muscles in individuals with muscular dystrophy or congenital myopathy were selected for full-length review. Data on the preferential involvement or sparing of individual muscles were extracted for analysis.

Results: 1937 publications were screened, 59 of which met the criteria for inclusion in the systematic review. There were 22 distinct genetic disorders represented in this analysis. In most studies, preferential involvement and sparing of specific muscles were reported.

Conclusions: MRI studies can identify distinct patterns of muscle involvement in the hereditary myopathies. Larger studies and standardized methods of reporting are needed to develop imaging as a diagnostic tool in these diseases.

Background

Since the introduction of clinical magnetic resonance imaging (MRI), investigators in the radiographic sciences have noted the ability of MRI to produce high-resolution anatomic images of skeletal muscle. Unlike prior imaging modalities, MRI provides excellent contrast between various soft tissue structures, allowing for the examination of individual muscles in sharp contrast to adjacent fat.[1] In recent years, MRI

of muscle has gained wider clinical use in the inflammatory myopathies, where the introduction of new immunosuppressive compounds has generated a need for tools that can accurately diagnose and monitor response to treatment. The ability of MRI to distinguish between acute inflammation and chronic fatty replacement of muscle also provides important prognostic information.[2]

In the muscular dystrophies and other hereditary myopathies, the clinical use of MRI as a diagnostic modality has not entered into the standard of care for multiple reasons. First, genetic testing has become increasingly available and affordable, and it offers highly specific diagnostic information that cannot be achieved with muscle imaging. The relative absence of large studies in this diverse patient population also makes the interpretation of MRI scans difficult. The absence of medical treatments for most hereditary muscle disorders also limits the utility of MRI, since imaging of muscle would not change the management of these conditions.

Despite the known limitations, there is growing interest in using imaging (and MRI in particular) in research studies of hereditary muscle disease.[3,4] Early trials in facioscapulohumeral muscular dystrophy (FSHD) have highlighted the limitations of existing outcome measures for muscular dystrophy.[5] An objective, non-invasive measure that can be repeated many times could significantly improve the quality of trials in these diseases.

The purpose of this review is to examine the methods with which researchers have used MRI to study genetic myopathies and to identify patterns of muscle involvement reported in the scientific literature. A systematic examination of the literature also provides an opportunity to identify obstacles that need to be addressed in the field of muscle imaging.

Methods

Literature searches

A search of the literature was performed in accordance with methods described by the Cochrane Handbook for Systematic Review of Interventions.[6] Controlled vocabulary and keyword searches were performed using the MEDLINE and EMBASE databases. Search terms were selected based on two concepts: 1) genetic muscle disease ("muscular dystrophy" or "congenital myopathy") and 2) magnetic resonance imaging ("magnetic resonance imaging" or "MRI" or "magnetic resonance spectroscopy" or "MRS"). We did not restrict our searches with regards to publication date, allowing searches to include all articles published from the time of database inception to the date of the literature search (1/26/2016). We further evaluated reference lists from included articles and completed forward citation searching using the Web of Science database to identify additional citations. Abbreviated search strategies were used to identify relevant information in the Cochrane Library, OpenSIGLE (System for Information on Grey Literature in Europe), and the New York Academy of Medicine Grey Literature Report and Database.

Study selection

All titles and abstracts were reviewed, and studies were excluded based on the following criteria: 1) the study was not performed in humans, 2) the study did not image skeletal muscles in at least one limb, 3) the study did not describe a genetically distinct muscular dystrophy, congenital myopathy, or distal myopathy, 4) the study did not isolate results of MRI studies from those of other imaging modalities, 5) the study described only a single kindred, 6) the study described fewer than four subjects, 7) the methods did not report or cite a system for scoring individual muscles based on fat infiltration, 8) the manuscript was a review or editorial publication that did not report primary research data, 9) the study was not published in English. The full-text versions

of studies that met these criteria based on titles and abstracts were downloaded and reviewed. Studies that did not meet these inclusion criteria after full-text review were subsequently excluded.

Data extraction and synthesis

The studies selected for analysis based on full-text review underwent data extraction. The following information about each study was collected: first author, year of publication, phenotype of study sample, genotype of study sample, number of MRI scans analyzed, regions imaged, and scoring system used for assessment of fat infiltration. Data on muscles that were preferentially affected and spared in each study population were also collected. Muscles were considered preferentially affected if they were defined by the authors as the earliest, most severely, or most frequently infiltrated by fat across the study sample. Muscles were considered preferentially spared if they were defined by the authors as relatively spared when compared to other muscles within an individual or were less frequently or severely involved across the study sample. The extracted data were stored in tabular form, with "+" signifying preferential involvement, "-" signifying sparing, "++" signifying the most preferentially involved muscle, and "--" signifying the most preferentially spared muscle. In instances where an entire muscle group was named instead of an individual muscle, all muscles within that group were coded equally. However, if regions comprised of more than one muscle group were named (for instance, "all pelvic muscles") and the muscles within those regions were not explicitly defined, these groups were not coded. In studies where multiple diseases were described, each genetically-distinct population that met the eligibility criteria was reported as a separate entry.

The degree of heterogeneity between studies was assessed through subgroup analyses in which studies were stratified by disease phenotype, genotype, scoring technique, sample size, and regions imaged.

Results

Search results and study selection

The search strategy identified 1937 unique citations (Figure 1).[7] Screening of titles and abstracts resulted in the exclusion of 1694 citations. A full-text review of the remaining 243 articles yielded 59 that were included in the final analysis. These studies were published between 1993 and 2016. Because some of these texts reported more than one genetic disease, there were 75 discrete disease populations ("cohorts") included in the analysis. These cohorts included a total of 1613 MRI scans.[8-66]

Characteristics of included studies

The included studies reported data from 22 different genetic myopathies (Table 1). The number of studies for each disease varied widely (range 1 to 16), with the dystrophinopathies and facioscapulohumeral muscular dystrophy (FSHD) accounting for the largest numbers of studies (16 and 13 studies respectively). The dystrophinopathies and FSHD each account for approximately one third of the scans described, and the remaining third was split among 20 different diseases. The number of scans analyzed in each study also varied widely (range 4 to 269). However, most cohorts were small (median 11 scans, mean 21.5 scans), and only three included more than 100 scans.

The majority of studies used a semi-quantitative scoring system with 4, 5, or 6 grades to rank individual muscles (Table 2). Higher numerical scores were used to signify more extensive fat infiltration. The specific muscle characteristics and cutoffs for each grade varied between studies; 25 cohorts were scored using a cutoff point of 50%

fat infiltration (similar to the scoring system described by Jungbluth) to denote changes in severity grade, and 29 cohorts were scored using cutoffs of 30% and 60% fat infiltration (similar to the Mercuri scale).[51, 56] Eight cohorts did not use specific cutoff percentages (like the Lamminen scale).[67] Only 13 of the 75 disease cohorts (8 dystrophinopathy, 3 FSHD, and 2 myotonic dystrophy) were analyzed using alternative scoring systems. Eight of these 13 cohorts were described in manuscripts published within the past five years and utilize fully quantitative methods of determining the amount of fat infiltration in muscle.

The majority of studies imaged the lower extremities, with 42 of the 75 cohorts exclusively imaging the lower extremities (lower leg, thigh, or pelvis). Thirty-two studies imaged the lower extremities and at least one other region of the body, and only two cohorts reported imaging of the upper extremities only. Seventeen cohorts (described in 11 separate manuscripts) reported using whole-body MRI, or scanning of contiguous anatomic regions that included the arms, trunk, and legs.

The dystrophinopathies

For the purposes of pattern analysis, dystrophinopathies were divided into 3 phenotypic subcategories (Duchenne, Becker, and carrier). While sharing a common genetic origin, the clinical features and natural history of these phenotypes vary widely. The Becker phenotype is milder than the Duchenne phenotype, while the majority of female carriers are asymptomatic. Despite these clinical disparities, the reported patterns of muscle involvement across all dystrophinopathies are similar, with at least half of studies reporting preferential involvement of the gluteus maximus, gluteus medius, and adductor magnus and sparing of the gracilis and sartorius (Table 3). The dystrophinopathy studies included the widest variety of scoring techniques for fat infiltration, with only about half using a semi-quantitative scoring system. The other

studies used fully quantitative techniques to characterize fat replacement. Five of these studies quantified the muscle fat fraction, or the percentage of muscle replaced by fat.

Facioscapulohumeral muscular dystrophy

Thirteen studies reported MRI findings in FSHD (Table 4). This group of studies showed the greatest anatomic diversity, with almost half of the studies imaging regions other than the legs. MRI of the arms is technically more challenging than imaging of the legs, and the number of studies that included upper extremity imaging likely reflects the high prevalence of upper extremity involvement in FSHD. A consistent finding among FSHD studies was the preferential involvement of the semimembranosus, which was reported to be the most severely involved muscle in nine of ten studies that scanned the thigh. The medial gastrocnemius and tibialis anterior muscles were the most preferentially affected in the lower leg, while the tibialis posterior and peroneus longus were frequently spared. The hip flexors (iliopsoas and iliacus) were preferentially spared in multiple studies. However, in contrast to Duchenne muscular dystrophy, the gracilis and sartorius were never reported to be preferentially spared. This may seem incongruous with prior observations of scans in which the gracilis and sartorius are spared relative to other muscles of the medial thigh in FSHD (Figure 2). One possible explanation is that only a subset of people with FSHD exhibit sparing of the gracilis and sartorius, and these muscles are not spared across the entire disease population.

Observations across all studies

Most genes had too few studies or were too heterogeneous to discern specific patterns of involvement (Tables 5-7). However, evaluation of imaging patterns across all 75 cohorts yielded several notable observations. Several muscles in the posterior compartment of the thigh (long head biceps femoris, semimembranosus), medial

compartment (adductor magnus), and lower leg (medial gastrocnemius, soleus) were the most likely to be preferentially involved across all studies. The gracilis, sartorius, and tibialis posterior were the most frequently spared. The rectus femoris, vastus lateralis, adductor longus, peroneus longus, and tibialis anterior showed a mix of preferential involvement and sparing in different diseases. In some cases, the preferential involvement or sparing was disease-specific. For instance, in studies describing FSHD, the tibialis anterior was reported to be preferentially involved, while the peroneus longus was found to be preferentially spared. In the dystrophinopathies, the reverse was true, with multiple studies reporting sparing of the tibialis anterior and involvement of the peroneus longus. In most other diseases and muscles, however, there were too few studies or scans to define a consistent pattern of involvement.

The diseases that were classified phenotypically as congenital myopathies or congenital muscular dystrophies showed distinct patterns of involvement compared to the dystrophinopathies, FSHD, limb-girdle muscular dystrophies, and distal myopathies. For instance, all of the diseases that reported preferential involvement of the sartorius were congenital myopathies or congenital muscular dystrophies. Similarly, the adductor longus was much more frequently spared in the congenital myopathies and congenital muscular dystrophies compared to the other forms of muscular dystrophy.

Some radiographic features that are specific to a particular disease were noted in this analysis. All of the studies describing collagen VI disorders reported that the outer rim of the vastus lateralis was preferentially affected before the center of the muscle. The majority of these studies also reported a strip or notch of fat replacement in the center of the rectus femoris.[47-49] Multiple studies describing type 1 myotonic dystrophy also reported a crescent-shaped pattern of involvement in the quadriceps resulting from greater involvement of the vastus intermedius and vastus medialis compared to the

vastus lateralis.[43,64,68] In the majority of studies, however, no similarly distinctive patterns of muscle involvement or disease-defining features were reported.

Discussion

This review emphasizes several important points about the role of MRI in the study of muscle disease. The identification of patterns of muscle involvement and sparing in different types of muscular dystrophy suggests that skeletal muscle imaging could be used in a diagnostic capacity. While MRI does not offer the specificity of gene testing, there are clinical scenarios where MRI could be diagnostically useful. For instance, MRI may be helpful in distinguishing hereditary from acquired myopathies, which could impact medical management considerably. It is also possible that muscle MRI will have a role in determining the pathogenicity of variants of unknown significance identified in through genetic testing.

The variability between studies of the same genetic disorder bears closer inspection. While the differences in reported patterns of muscle involvement are likely due in part to differences in scoring and reporting techniques, other sources of variability should also be considered. The increasing use of genetic testing has shown that in many genetic diseases, the phenotypic variability is far wider than was previously suspected. A number of genes, such as collagen VI and dysferlin, are associated with more than 1 clinical phenotype.[42,47] In FSHD, genotyping of family members has shown that some individuals who carry a disease-causing mutation are either asymptomatic or minimally affected.[69,70] It is therefore possible that contradictory findings in imaging studies could relate to distinct subgroups within a disease population.

The results of this analysis also show that the field of MRI in muscular dystrophy is dominated by the dystrophinopathies and FSHD. This likely reflects not only the relative frequency of these disorders, but the activity of subspecialty research centers,

patient registries, and advocacy groups. The relative paucity of scans in other diseases compels caution in drawing conclusions about the patterns of muscle involvement in these disorders, as small studies in selected populations may be subject to selection bias. In the extremely rare muscular dystrophies, the collection of sufficient numbers of scans to adequately characterize the disease population may only be achievable through collaborations between multiple centers around the world.

There are some important limitations to this qualitative review. First, this review does not discriminate between different types of preferential involvement or sparing. Preferential involvement could mean the most frequently affected, the earliest affected, or the most extensively fat replaced muscle. Likewise, preferential sparing could mean that a muscle is universally spared across the cohort or relatively spared compared to other muscles in the same person. We relied on the authors to report preferentially involved or spared muscles in cases where the primary data were not provided in the manuscript text, and the criteria for identifying these muscles was infrequently reported. Despite these potential inconsistencies, the reported patterns of fat infiltration within individual diseases are reasonably consistent. In future observational studies and clinical trials, however, it will be essential to develop a uniform system of classifying and reporting imaging findings.

Some hereditary myopathies were not included in this review, namely, the metabolic myopathies, mitochondrial myopathies, and non-dystrophic myotonias (the muscle ion channel disorders). While imaging studies have been performed in these disorders, fat replacement of muscle is not a universally reported feature in these diseases, and appropriate comparisons with regards to preferential muscle involvement could not be made.[71-74]

Another potential limitation is that we were unable to stratify imaging findings based on important disease-modifying factors in muscular dystrophy, such as gender,

age of onset (or duration of symptoms), age, or mutation type. At least one of the included studies reported differences in the patterns of muscle involvement between males and females.[44] Our analysis also only included data on fat infiltration and did not take into account other features of muscle disease, such as edema-like changes, muscle hypertrophy, or atrophy. These factors could denote important disease subgroups and merit further characterization in future studies.

The results of this review underline several factors that should be considered in studies using MRI in muscle disease. First is the need for greater standardization across all stages of imaging, from the selection of participants and imaging sequences to the scoring and reporting of collected images. Standardized methodologies will facilitate the extraction and synthesis of findings across multiple investigator groups.[75] Secondly, the radiographic phenotypes of muscle diseases can differ considerably from clinical observations. For instance, several studies reported that the medial gastrocnemius muscle is as frequently or more frequently affected than the tibialis anterior in FSHD. However, foot drop is more frequently observed than calf weakness in this disease population. This may be due to the fact that there are multiple muscles involved in ankle plantarflexion, all of which are larger than the tibialis anterior. Extensive replacement of a single muscle may not be clinically apparent if other members of the same muscle group remain intact. It is also important to consider that the majority of these studies are fairly small case series in which a well-defined clinical population was imaged. In these cases, it could be expected that imaging findings would be more homogeneous. As imaging studies expand to include more atypical cases, we would expect the radiographic phenotypes of these disorders to be more heterogeneous as well.

References

1. Murphy WA, Totty WG, Carroll JE. MRI of normal and pathologic skeletal muscle. AJR Am J Roentgenol 1986;146:565-74.

2. Del Grande F, Carrino JA, Del Grande M, Mammen AL, Christopher Stine L. Magnetic resonance imaging of inflammatory myopathies. Topics in magnetic resonance imaging : TMRI 2011;22:39-43.

3. Mercuri E, Pichiecchio A, Allsop J, Messina S, Pane M, Muntoni F. Muscle MRI in inherited neuromuscular disorders: past, present, and future. Journal of magnetic resonance imaging : JMRI 2007;25:433-40.

4. Wattjes MP, Kley RA, Fischer D. Neuromuscular imaging in inherited muscle diseases. Eur Radiol 2010;20:2447-60.

5. Tawil R, Padberg GW, Shaw DW, van der Maarel SM, Tapscott SJ, Participants FW. Clinical trial preparedness in facioscapulohumeral muscular dystrophy: Clinical, tissue, and imaging outcome measures 29-30 May 2015, Rochester, New York. Neuromuscular disorders : NMD 2016;26:181-6.

6. Higgins JPT, Green S, Cochrane Collaboration. Cochrane handbook for systematic reviews of interventions. Chichester, England ; Hoboken, NJ: Wiley-Blackwell; 2008.

7. Moher D, Liberati A, Tetzlaff J, Altman DG, Group P. Preferred reporting items for systematic reviews and meta-analyses: the PRISMA statement. J Clin Epidemiol 2009;62:1006-12.

8. Faridian-Aragh N, Wagner KR, Leung DG, Carrino JA. Magnetic resonance imaging phenotyping of Becker muscular dystrophy. Muscle Nerve 2014;50:962-7.

9. Tasca G, Iannaccone E, Monforte M, et al. Muscle MRI in Becker muscular dystrophy. Neuromuscular disorders : NMD 2012;22 Suppl 2:S100-6.

10. Loughran T, Higgins DM, McCallum M, Coombs A, Straub V, Hollingsworth KG. Improving highly accelerated fat fraction measurements for clinical trials in muscular dystrophy: origin and quantitative effect of R2* changes. Radiology 2015;275:570-8.

11. van den Bergen JC, Wokke BH, Janson AA, et al. Dystrophin levels and clinical severity in Becker muscular dystrophy patients. Journal of neurology, neurosurgery, and psychiatry 2014;85:747-53.

12. Tasca G, Monforte M, Iannaccone E, et al. Muscle MRI in female carriers of dystrophinopathy. Eur J Neurol 2012;19:1256-60.

13. Kim HK, Laor T, Horn PS, Racadio JM, Wong B, Dardzinski BJ. T2 mapping in Duchenne muscular dystrophy: distribution of disease activity and correlation with clinical assessments. Radiology 2010;255:899-908.

14. Gaeta M, Messina S, Mileto A, et al. Muscle fat-fraction and mapping in Duchenne muscular dystrophy: Evaluation of disease distribution and correlation with clinical assessments preliminary experience. Skeletal radiology 2012;41:955-61.

15. Kim HK, Merrow AC, Shiraj S, Wong BL, Horn PS, Laor T. Analysis of fatty infiltration and inflammation of the pelvic and thigh muscles in boys with Duchenne muscular dystrophy (DMD): grading of disease involvement on MR imaging and correlation with clinical assessments. Pediatr Radiol 2013;43:1327-35.

16. Liu GC, Jong YJ, Chiang CH, Jaw TS. Duchenne muscular dystrophy: MR grading system with functional correlation. Radiology 1993;186:475-80.

17. Garrood P, Hollingsworth KG, Eagle M, et al. MR imaging in Duchenne muscular dystrophy: quantification of T1-weighted signal, contrast uptake, and the effects of exercise. Journal of magnetic resonance imaging : JMRI 2009;30:1130-8.

18. Li W, Zheng Y, Zhang W, Wang Z, Xiao J, Yuan Y. Progression and variation of fatty infiltration of the thigh muscles in Duchenne muscular dystrophy, a muscle magnetic resonance imaging study. Neuromuscular disorders : NMD 2015;25:375-80.

19. Ponrartana S, Ramos-Platt L, Wren TAL, et al. Effectiveness of diffusion tensor imaging in assessing disease severity in Duchenne muscular dystrophy: preliminary study. Pediatric radiology 2014.

20. Wokke BH, van den Bergen JC, Versluis MJ, et al. Quantitative MRI and strength measurements in the assessment of muscle quality in Duchenne muscular dystrophy. Neuromuscular disorders : NMD 2014;24:409-16.

21. Kinali M, Arechavala-Gomeza V, Cirak S, et al. Muscle histology vs MRI in Duchenne muscular dystrophy. Neurology 2011;76:346-53.

22. Torriani M, Townsend E, Thomas BJ, Bredella MA, Ghomi RH, Tseng BS. Lower leg muscle involvement in Duchenne muscular dystrophy: an MR imaging and spectroscopy study. Skeletal Radiol 2012;41:437-45.

23. Vohra RS, Lott D, Mathur S, et al. Magnetic Resonance Assessment of Hypertrophic and Pseudo-Hypertrophic Changes in Lower Leg Muscles of Boys with Duchenne Muscular Dystrophy and Their Relationship to Functional Measurements. PLoS ONE 2015;10:e0128915.

24. Tasca G, Monforte M, Iannaccone E, et al. Upper girdle imaging in facioscapulohumeral muscular dystrophy. PLoS ONE 2014;9:e100292.

25. Jordan B, Eger K, Koesling S, Zierz S. Camptocormia phenotype of FSHD: a clinical and MRI study on six patients. J Neurol 2011;258:866-73.

26. Regula JU, Jestaedt L, Jende F, Bartsch A, Meinck HM, Weber MA. Clinical Muscle Testing Compared with Whole-Body Magnetic Resonance Imaging in Facio-scapulo-humeral Muscular Dystrophy. Clin Neuroradiol 2015.

27. Gerevini S, Scarlato M, Maggi L, et al. Muscle MRI findings in facioscapulohumeral muscular dystrophy. European radiology 2015.

28. Leung DG, Carrino JA, Wagner KR, Jacobs MA. Whole-body magnetic resonance imaging evaluation of facioscapulohumeral muscular dystrophy. Muscle Nerve 2015;52:512-20.

29. Rijken NH, van Engelen BG, de Rooy JW, Geurts AC, Weerdesteyn V. Trunk muscle involvement is most critical for the loss of balance control in patients with facioscapulohumeral muscular dystrophy. Clinical biomechanics (Bristol, Avon) 2014;29:855-60.

30. Olsen DB, Gideon P, Jeppesen TD, Vissing J. Leg muscle involvement in facioscapulohumeral muscular dystrophy assessed by MRI. J Neurol 2006;253:1437-41.

31. Iosa M, Mazza C, Frusciante R, et al. Mobility assessment of patients with facioscapulohumeral dystrophy. Clinical biomechanics (Bristol, Avon) 2007;22:1074-82.

32. Tasca G, Monforte M, Ottaviani P, et al. Magnetic Resonance Imaging in a large cohort of facioscapulohumeral muscular dystrophy patients: pattern refinement and implications for clinical trials. Annals of neurology 2016.

33. Janssen BH, Voet NB, Nabuurs CI, et al. Distinct disease phases in muscles of facioscapulohumeral dystrophy patients identified by MR detected fat infiltration. PLoS ONE 2014;9:e85416.

34. Lareau-Trudel E, Troter AL, Ghattas B, et al. Muscle quantitative MR imaging and clustering analysis in patients with facioscapulohumeral muscular dystrophy type 1. PLoS ONE 2015;10.

35. Kan HE, Klomp DW, Wohlgemuth M, et al. Only fat infiltrated muscles in resting lower leg of FSHD patients show disturbed energy metabolism. NMR Biomed 2010;23:563-8.

36. Friedman SD, Poliachik SL, Carter GT, Budech CB, Bird TD, Shaw DW. The magnetic resonance imaging spectrum of facioscapulohumeral muscular dystrophy. Muscle Nerve 2012;45:500-6.

37. Stramare R, Beltrame V, Dal Borgo R, et al. MRI in the assessment of muscular pathology: a comparison between limb-girdle muscular dystrophies, hyaline body myopathies and myotonic dystrophies. La Radiologia medica 2010;115:585-99.

38. Fischer D, Walter MC, Kesper K, et al. Diagnostic value of muscle MRI in differentiating LGMD2I from other LGMDs. J Neurol 2005;252:538-47.

39. Mercuri E, Bushby K, Ricci E, et al. Muscle MRI findings in patients with limb girdle muscular dystrophy with calpain 3 deficiency (LGMD2A) and early contractures. Neuromuscular disorders : NMD 2005;15:164-71.

40. Kesper K, Kornblum C, Reimann J, Lutterbey G, Schroder R, Wattjes MP. Pattern of skeletal muscle involvement in primary dysferlinopathies: a whole-body 3.0-T magnetic resonance imaging study. Acta Neurol Scand 2009;120:111-8.

41. Diaz J, Woudt L, Suazo L, et al. Broadening The Imaging Phenotype of Dysferlinopathy at Different Disease Stages. Muscle & nerve 2016.

42. Paradas C, Llauger J, Diaz-Manera J, et al. Redefining dysferlinopathy phenotypes based on clinical findings and muscle imaging studies. Neurology 2010;75:316-23.

43. Degardin A, Morillon D, Lacour A, Cotten A, Vermersch P, Stojkovic T. Morphologic imaging in muscular dystrophies and inflammatory myopathies. Skeletal Radiol 2010;39:1219-27.

44. Willis TA, Hollingsworth KG, Coombs A, et al. Quantitative magnetic resonance imaging in limb-girdle muscular dystrophy 2I: a multinational cross-sectional study. PLoS ONE 2014;9:e90377.

45. Mahjneh I, Bashir R, Kiuru-Enari S, Linssen W, Lamminen A, Visser M. Selective pattern of muscle involvement seen in distal muscular dystrophy associated with anoctamin 5 mutations: a follow-up muscle MRI study. Neuromuscular disorders : NMD 2012;22 Suppl 2:S130-6.

46. Sarkozy A, Deschauer M, Carlier RY, et al. Muscle MRI findings in limb girdle muscular dystrophy type 2L. Neuromuscular disorders : NMD 2012;22 Suppl 2:S122-9.

47. Mercuri E, Lampe A, Allsop J, et al. Muscle MRI in Ullrich congenital muscular dystrophy and Bethlem myopathy. Neuromuscular disorders : NMD 2005;15:303-10.

48. Quijano-Roy S, Avila-Smirnow D, Carlier RY, group W-Mms. Whole body muscle MRI protocol: pattern recognition in early onset NM disorders. Neuromuscular disorders : NMD 2012;22 Suppl 2:S68-84.

49. Mercuri E, Cini C, Pichiecchio A, et al. Muscle magnetic resonance imaging in patients with congenital muscular dystrophy and Ullrich phenotype. Neuromuscular disorders : NMD 2003;13:554-8.

50. Gomez-Andres D, Dabaj I, Mompoint D, et al. Pediatric laminopathies: Whole-body MRI fingerprint and comparison with SEPN1-myopathy. Muscle & nerve 2015.

51. Mercuri E, Counsell S, Allsop J, et al. Selective muscle involvement on magnetic resonance imaging in autosomal dominant Emery-Dreifuss muscular dystrophy. Neuropediatrics 2002;33:10-4.

52. Carboni N, Mura M, Marrosu G, et al. Muscle imaging analogies in a cohort of patients with different clinical phenotypes caused by LMNA gene mutations. Muscle Nerve 2010;41:458-63.

53. Hankiewicz K, Carlier RY, Lazaro L, et al. Whole-body muscle magnetic resonance imaging in SEPN1-related myopathy shows a homogeneous and recognizable pattern. Muscle & nerve 2015;52:728-35.

54. Jungbluth H, Davis MR, Muller C, et al. Magnetic resonance imaging of muscle in congenital myopathies associated with RYR1 mutations. Neuromuscular disorders : NMD 2004;14:785-90.

55. Jarraya M, Quijano-Roy S, Monnier N, et al. Whole-Body muscle MRI in a series of patients with congenital myopathy related to TPM2 gene mutations. Neuromuscular disorders : NMD 2012;22 Suppl 2:S137-47.

56. Jungbluth H, Sewry CA, Counsell S, et al. Magnetic resonance imaging of muscle in nemaline myopathy. Neuromuscular disorders : NMD 2004;14:779-84.

57. Schramm N, Born C, Weckbach S, Reilich P, Walter MC, Reiser MF. Involvement patterns in myotilinopathy and desminopathy detected by a novel neuromuscular whole-body MRI protocol. Eur Radiol 2008;18:2922-36.

58. McNeill A, Birchall D, Straub V, et al. Lower limb radiology of distal myopathy due to the S60F myotilin mutation. Eur Neurol 2009;62:161-6.

59. Muller TJ, Kraya T, Stoltenburg-Didinger G, et al. Phenotype of matrin-3-related distal myopathy in 16 German patients. Ann Neurol 2014;76:669-80.

60. Mahjneh I, Lamminen AE, Udd B, et al. Muscle magnetic resonance imaging shows distinct diagnostic patterns in Welander and tibial muscular dystrophy. Acta Neurol Scand 2004;110:87-93.

61. Fischmann A, Gloor M, Fasler S, et al. Muscular involvement assessed by MRI correlates to motor function measurement values in oculopharyngeal muscular dystrophy. J Neurol 2011;258:1333-40.

62. Zhao J, Liu J, Xiao J, et al. Clinical and muscle imaging findings in 14 mainland chinese patients with oculopharyngodistal myopathy. PLoS ONE 2015;10:e0128629.

63. Sugie K, Sugie M, Taoka T, et al. Characteristic MRI Findings of upper Limb Muscle Involvement in Myotonic Dystrophy Type 1. PloS one 2015;10:e0125051.

64. Kornblum C, Lutterbey G, Bogdanow M, et al. Distinct neuromuscular phenotypes in myotonic dystrophy types 1 and 2 : a whole body highfield MRI study. J Neurol 2006;253:753-61.

65. Damian MS, Bachmann G, Herrmann D, Dorndorf W. Magnetic resonance imaging of muscle and brain in myotonic dystrophy. J Neurol 1993;240:8-12.

66. Hamano T, Kawamura Y, Mutoh T, Hirayama M, Kuriyama M. Muscle MRI in myotonic dystrophy type 1 with foot drop. Eur Neurol 2010;63:144-8.

67. Lamminen AE. Magnetic resonance imaging of primary skeletal muscle diseases: patterns of distribution and severity of involvement. The British journal of radiology 1990;63:946-50.

68. Stramare R, Beltrame V, Dal Borgo R, et al. MRI in the assessment of muscular pathology: a comparison between limb-girdle muscular dystrophies, hyaline body myopathies and myotonic dystrophies. Radiologia Medica 2010:1-15.

69. Sakellariou P, Kekou K, Fryssira H, et al. Mutation spectrum and phenotypic manifestation in FSHD Greek patients. Neuromuscular disorders : NMD 2012;22:339-49.

70. Lin F, Wang ZQ, Lin MT, Murong SX, Wang N. New Insights into Genotype-phenotype Correlations in Chinese Facioscapulohumeral Muscular Dystrophy: A Retrospective Analysis of 178 Patients. Chin Med J (Engl) 2015;128:1707-13.

71. Morrow JM, Matthews E, Raja Rayan DL, et al. Muscle MRI reveals distinct abnormalities in genetically proven non-dystrophic myotonias. Neuromuscular disorders : NMD 2013;23:637-46.

72. Kornblum C, Lutterbey GG, Czermin B, et al. Whole-body high-field MRI shows no skeletal muscle degeneration in young patients with recessive myotonia congenita. Acta Neurol Scand 2010;121:131-5.

73. Horvath JJ, Austin SL, Case LE, et al. Correlation between quantitative whole-body muscle magnetic resonance imaging and clinical muscle weakness in Pompe disease. Muscle & nerve 2015;51:722-30.

74. Olsen DB, Langkilde AR, Orngreen MC, Rostrup E, Schwartz M, Vissing J. Muscle structural changes in mitochondrial myopathy relate to genotype. J Neurol 2003;250:1328-34.

75. Hollingsworth KG, de Sousa PL, Straub V, Carlier PG. Towards harmonization of protocols for MRI outcome measures in skeletal muscle studies: consensus recommendations from two TREAT-NMD NMR workshops, 2 May 2010, Stockholm, Sweden, 1-2 October 2009, Paris, France. Neuromuscular disorders : NMD 2012;22 Suppl 2:S54-67.

Table 1: Numbers of studies and scans for genetic disorders included in systematic review.

Gene		Number of studies	Total number of scans	Percentage of studies	Percentage of scans
ACTA1		1	4	1.3%	0.2%
COL6		4	47	5.3%	2.9%
DES		1	4	1.3%	0.2%
DMPK		6	80	8.0%	5.0%
CNBP		3	23	4.0%	1.4%
DMD					
	Duchenne	11	411	14.7%	25.5%
	Becker	4	96	5.3%	6.0%
	Carrier	1	12	1.3%	0.7%
FSHD		13	586	17.3%	36.3%
CAPN		3	22	4.0%	1.4%
DYSF		5	83	6.7%	5.1%
FKRP		3	51	4.0%	3.2%
ANO5		2	30	2.7%	1.9%
LMNA		4	38	5.3%	2.4%
MATR3		1	16	1.3%	1.0%
MYOT		2	13	2.7%	0.8%
NEB		1	6	1.3%	0.4%
PABN		2	18	2.7%	1.1%
RYR1		2	15	2.7%	0.9%
SEPN1		2	13	2.7%	0.8%
TTN		1	22	1.3%	1.4%
TPM2		2	12	2.7%	0.7%
TIA1		1	11	1.3%	0.7%
Total		**75**	**1613**		

Table 2: The majority of studies selected for review used a variant of one of the following three scoring systems.

Score	Lamminen 1990	Mercuri 2002	Jungbluth 2004
0		normal	normal
1	normal muscle signal intensity	early moth-eaten appearance, with scattered small areas of increased density on T1 MRI	mild with only traces of increased signal intensity
2	slighty hyperintense, patchy intramuscular signal changes	a: late moth-eaten appearance, with numerous discrete areas of increased density with beginning confluence, comprising less than 30% of the volume of the individual muscle	moderate with increased signal in less than 50% of affected muscle
		b: late moth-eaten appearance, with numerous discrete areas of increased density with beginning confluence, comprising 30-60% of the volume of the individual muscle	
3	markedly hyperintese, patchy but widespread intramuscular changes	washed-out appearance, fuzzy appearance due to confluent areas of increased density with muscle still present at the periphery	severe with increased signal intensity in more than 50% of affected muscle
4	total, homogeneous hyperintense signal change in whole muscle, equaling the signal intensity of adjacent subcutaneous or paramuscular fat	end-stage appearance, muscle replaced by increased density connective tissue and fat with only rim of fascia and neurovascular structures distinguishable	entire muscle replaced by abnormal signal

Table 3: Patterns of muscle involvement and sparing in MRI studies describing populations with dystrophinopathies.

Author	Year	Phenotype	Number of scans	Regions imaged	Scoring	medial gastrocnemius	lateral gastrocnemius	soleus	tibialis anterior	peroneus	popliteus	tibialis posterior	extensor digitorum longus	biceps femoris, long head	biceps femoris, short head	semimembranosus	semitendinosus	adductor magnus	adductor longus	rectus femoris	vastus lateralis	vastus medialis	vastus intermedius	sartorius	gracilis	gluteus maximus	gluteus medius	obturator externus	iliopsoas	iliacus	quadratus femoris	paraspinal	rectus abdominis	teres major	deltoid	biceps brachii	triceps
Faridian-Aragh	2014	Becker	33	arm, upper leg, lower leg	5 grades									+	+	+	+	+	+	+	+	+	+	-		+	+	-						+	-	+	+
Tasca	2012	Becker	46	upper leg, lower leg, pelvis	5 grades						-	-		+		+		+			+	+	+			+	+		-								
Loughran	2015	Becker	8	upper leg, lower leg	Muscle fat fraction				-					+																							
VandenBergen	2014	Becker	9	lower leg	Muscle fat fraction	++	+		-	+																											
Tasca	2012	Carriers	12	upper leg, lower leg, pelvis	5 grades						-			+				+			+	+	+	-	-	+	+		-		+	+	-				
Kim	2010	Duchenne	34	upper leg, pelvis	5 grades																				--	++											
Gaeta	2012	Duchenne	20	upper leg, pelvis	Muscle fat fraction												-	+							--	++											
Kim	2013	Duchenne	42	upper leg, pelvis	5 grades													+						-	--	++	+			-							
Liu	1993	Duchenne	29	upper leg, lower leg, pelvis	0-10 point scale											-	-							-	--												
Garrood	2009	Duchenne	11	upper leg, lower leg, pelvis	Median signal intensity									+				+	+	+						+											
Li	2015	Duchenne	171	upper leg	6 grades									+	+			+	-					-	-	+											
Ponrartana	2014	Duchenne	13	upper leg, lower leg	Muscle fat fraction					+		-												-		+											
Wokke	2014	Duchenne	16	upper leg, lower leg	Muscle fat fraction	+	+			+				+				++		+	+	+	+														
Kinali	2011	Duchenne	34	lower leg	6 grades	+	+		-		-	-	-																								
Torriani	2012	Duchenne	9	lower leg	5 grades	+		+		++		--																									
Vohra	2015	Duchenne	32	lower leg	Cross-sectional area	++			-				-																								

Table 4: Patterns of muscle involvement and sparing in MRI studies describing facioscapulohumeral muscular dystrophy.

Author	Year	Number of scans	Regions imaged	Scoring	medial gastrocnemius	lateral gastrocnemius	tibialis anterior	peroneus	popliteus	tibialis posterior	extensor digitorum longus	flexor digitorum	biceps femoris, long head	biceps femoris, short head	semimembranosus	semitendinosus	adductor magnus	adductor longus	adductor brevis	rectus femoris	vastus lateralis	vastus medialis	vastus intermedius	gluteus maximus	gluteus medius	gluteus minimus	obturator externus	obturator internus	tensor fasciae latae	iliopsoas	iliacus	quadratus lumborum	paraspinal	rectus abdominis	obliques	latissimus	trapezius	pectoralis major	serratus anterior	scalene	subscapularis	supraspinatus	infraspinatus	teres minor	teres major
Tasca	2014	108	shoulder	4 grades																															+	+	+	+		-	-	-		
Jordan	2011	6	shoulder, trunk, pelvis, upper leg, lower leg	5 grades	+	+									++		+	+	+					+	+	+				-		-	+			+								
Regula	2015	20	whole-body	4 grades											++		+	+															+	+			+		+						
Gerevini	2015	30	whole-body	4 grades						-					++									+		+		-		-	-			+		+		+	-		-	-		+
Leung	2015	13	whole-body	6 grades					-	-			+	+	++	+		+		+					+	+	-	-	+		-		+	+		+		+	+		-	-	-	-	
Rijken	2014	10	trunk, upper leg, lower leg	4 grades	+		+						+	+	++	+				+													+	+										
Olsen	2006	18	upper leg, lower leg, pelvis	4 grades	+		+	-					+	+	++	+	+	+	+		-	-	-	-	-	-				--														
Iosa	2007	12	upper leg, lower leg, pelvis	4 grades	+		+								++						+	+	+																					
Tasca	2016	269	upper leg, lower leg, pelvis	5 grades					-	-		-	+		+											+	-	-		-				+										
Janssen	2014	41	upper leg	Muscle fat fraction											++	+	+	+		+	-		-																					
Lareau-Trudel	2015	35	upper leg, lower leg	4 grades	+		+	-		-			+	+	++	+	+	+	+																									
Kan	2010	9	lower leg	2 grades	++		+	-		-	+																																	
Friedman	2012	15	lower leg	Muscle/fat ratio	+	+	+			-																																		

Table 5: Patterns of muscle involvement and sparing in MRI studies describing limb-girdle muscular dystrophy. M and F denote findings seen only in males or females, respectively.

Author	Year	Genotype	Number of scans	Regions imaged	Scoring	medial gastrocnemius	lateral gastrocnemius	soleus	tibialis anterior	peroneus	popliteus	tibialis posterior	extensor digitorum longus	flexor hallucis longus	biceps femoris, long head	biceps femoris, short head	semimembranosus	semitendinosus	adductor magnus	adductor longus	adductor brevis	rectus femoris	vastus lateralis	vastus medialis	vastus intermedius	sartorius	gluteus maximus	gluteus medius	gluteus minimus	obturator externus	obturator internus	pectineus	tensor fasciae latae	iliopsoas	piriformis	paraspinal	rectus abdominis	obliques	pectoralis minor	serratus anterior	subscapularis	supraspinatus	infraspinatus	teres major	coracobrachialis	levator scapulae	brachioradialis	biceps brachii	triceps	flexor digitorum	flexor pollucis longus	sternocleidomastoid
Stramare	2010	LGMD2A	10	shoulder, pelvis, upper leg, lower leg	6 grades							-			+	+	+	+	+	+	+				-	-																								
Fischer	2005	LGMD2A	5	upper leg, lower leg, pelvis	6 grades	+	-	+							+	+	+		+			-	-	-	-				+																							
Mercuri	2005	LGMD2A	7	upper leg, lower leg	4 grades	+	-		-	-							+		+				-		+	-	-						-																		
Stramare	2010	LGMD2B	16	shoulder, pelvis, upper leg, lower leg	6 grades	+	+	+		+		+			+	+	+	+	+	+	+					-	-		+				+																		
Kesper	2009	LGMD2B	6	whole-body	5 grades	-	+		+	+					+	+	+		+				+	+	+	-	-			+						+															
Diaz	2016	LGMD2B	27	whole-body	5 grades	+	+	+			-			+	+	+	+	+	+	+	+					-	-			+				-	+		+	-		+					-	+	+	-
Fischer	2005	LGMD2B	5	upper leg, lower leg, pelvis	6 grades	+	+	+							+	+	+		+				+	+	+			+	+																						
Paradas	2010	LGMD2B	29	upper leg, lower leg	4 grades	+	+	+				-			-	-	+		+			-	+			-	-																								
Degardin	2010	LGMD2I	7	shoulder, pelvis, upper leg, lower leg	4 grades										+	+	+	+	+	+	+	-				-	-			+	+	+							+	+	+	+						-			
Fischer	2005	LGMD2I	6	upper leg, lower leg, pelvis	6 grades	+		+							+	+	+		+			-		-				+																							
Willis	2014	LGMD2I	38	upper leg, lower leg	6 grades	+	+ F	+	-						++		+ M	+				-	-	+ M		- F	-	+																							
Mahjneh	2012	LGMD2L	5	upper leg, lower leg, pelvis	4 grades	+		+																				-																							
Sarkozy	2012	LGMD2L	25	upper leg, lower leg, pelvis	4 grades	+	+	+	-				-		-	-	+	+	+	+		-				-	-	-	-	-																						

Table 6: Patterns of muscle involvement and sparing in MRI studies describing congenital myopathy, congenital muscular dystrophy (CMD), Emery-Dreifuss muscular dystrophy (EDMD), distal myopathy, and oculopharyngeal muscular dystrophy (OPMD). A * denotes fat replacement in the center of the muscle. A ± denotes fat replacement at the muscle periphery.

Author	Year	Genotype	Phenotype	Number of scans	Regions imaged	Scoring	medial gastrocnemius	lateral gastrocnemius	soleus	tibialis anterior	peroneus	popliteus	tibialis posterior	extensor digitorum longus	extensor hallucis longus	flexor digitorum	biceps femoris, long head	biceps femoris, short head	semimembranosus	semitendinosus	adductor magnus	adductor longus	adductor brevis	rectus femoris	vastus lateralis	vastus medialis	vastus intermedius	sartorius	gracilis	gluteus maximus	gluteus medius	gluteus minimus	tensor fasciae latae	iliopsoas	iliacus	paraspinal	rectus abdominis	intercostal	latissimus	rhomboid	serratus anterior	subscapularis	deltoid	levator scapulae	biceps brachii	triceps	sternocleidomastoid	longus colli	temporalis	pterygoid	intrinsic tongue muscles	masseter
Mercuri	2005	COL6	CMD - Bethlem	10	upper leg, lower leg	4 grades	±	±	±	-		-										-		*	±			-	-																					
Quijano-Roy	2012	COL6	CMD - Bethlem/Ullrich	13	whole-body	4 grades	±	±	±	-												-		*	±			-	-	±					±							±	±			±					
Mercuri	2003	COL6	CMD - Ullrich	15	upper leg, lower leg, pelvis	6 grades				-		-										-			±			-	-																							
Mercuri	2005	COL6	CMD - Ullrich	9	upper leg, lower leg	4 grades	+	+	+	-		-										-		*	±			-	-																							
Gomez-Andres	2015	LMNA	CMD	8	whole-body	4 grades	+		+				-			-		-	+		+	+		-	+	+	+	-	-	-	+	+			+	-				+	+		-			-	+				
Quijano-Roy	2012	LMNA	CMD, EDMD	4	whole-body	4 grades	+			-	-		-	-		-	+	+	+	+	+			-	+	+	+	-	-		+	+			+	-															
Mercuri	2002	LMNA	EDMD	9	upper leg, lower leg	4 grades	++	-																																												
Carboni	2010	LMNA	EDMD, cardiac disorders	17	upper leg, lower leg	4 grades	+		+																																										
Quijano-Roy	2012	SEPN1	congenital myopathy	4	whole-body	4 grades											+	+	+			-		-				+	-	+						+	+									+					
Hankiewicz	2015	SEPN1	congenital myopathy	9	whole-body	4 grades				-			-					+	+	-	+	-			-				+	-	+				-	+								-								
Jungbluth	2004	RYR1	congenital myopathy	11	upper leg, lower leg	5 grades	+	+	+	-	+										+	-		-	+	+	+	+	-																						
Quijano-Roy	2012	RYR1	congenital myopathy	4	whole-body	4 grades	-	-	+	-	-		+			+			+		+	-		-	+	+			-	+	+	+		+		+	+	+	+					+		-			-		
Jarraya	2012	TPM2	congenital myopathy	8	whole-body	4 grades			++	+	+					+	+				-	-			+			-																					+	+	-	
Quijano-Roy	2012	TPM2	congenital myopathy	4	whole-body	4 grades		+	+		+			+										+																										+			+
Jungbluth	2004	ACTA1	congenital myopathy	4	upper leg, lower leg, pelvis	5 grades	-	-																				+	-																							
Jungbluth	2004	NEB	congenital myopathy	6	upper leg, lower leg, pelvis	5 grades	-	-	+	+	-		-																																							
Schramm	2008	DES	myofibrillar myopathy	4	whole-body	4 grades	+		+	+	+		+						-	+				-	+	+	+	+	+					+																	
Schramm	2008	MYOT	myofibrillar myopathy	5	whole-body	4 grades	+		+	+	+		+				+	+	+	-	+	+		-					-	+	+	+			+				+											
McNeill	2009	MYOT	distal myopathy	8	upper leg, lower leg	4 grades	+	-	+	+	+	-	+	+	+		+	+	+	+					-	+	+	-	-																					
Muller	2014	MATR3	distal myopathy	16	trunk, upper leg, lower leg	5 grades	+		+				-						+					-	-	-	-																							
Mahjneh	2004	TIA1	distal myopathy	11	upper leg, lower leg	4 grades	+	+	+	+			+				+	+	+	+	+																														
Mahjneh	2004	TTN	distal myopathy	22	upper leg, lower leg	4 grades				+	-		+				+			+				-	-																										
Fischmann	2011	PABPN1	OPMD	8	upper leg, lower leg	4 grades	+		+	-							+	+	+		++					-		-	-																						
Zhao	2015	PABPN1	OPMD	10	upper leg, lower leg	6 grades	+	+	++		+	-		+			+	-	+		+			-	+	+	+	-	-																						

Table 7: Patterns of muscle involvement and sparing in MRI studies describing myotonic dystrophy.

Author	Year	Genotype	Number of scans	Regions image	Scoring	medial gastrocnemius	lateral gastrocnemius	soleus	tibialis anterior	peroneus	tibialis posterior	biceps femoris, long head	biceps femoris, short head	semimembranosus	semitendinosus	adductor magnus	adductor longus	adductor brevis	rectus femoris	vastus lateralis	vastus medialis	vastus intermedius	sartorius	gracilis	gluteus maximus	gluteus minimus	obturator externus	obturator internus	paraspinal	biceps brachii	triceps	flexor digitorum	extensor digitorum	flexor pollucis longus	abductor pollucis longus	extensor pollucis	flexor carpi	extensor carpi
Sugie	2015	DM1	17	arm	5 grades																								+	+	++	-	+	+	+	-	-
Kornblum	2006	DM1	15	whole-body	5 grades	++		+			-								-		+																	
Stramare	2010	DM1	6	shoulder, arm, pelvis, upper leg, lower leg	6 grades	+	+	+		+	-								-	-	+	+	-								+	+					
Degardin	2010	DM1	4	shoulder, pelvis, upper leg, lower leg	4 grades	+			+		-								+	+	+	+							+									
Damian	1993	DM1	25	upper leg, lower leg	0-5 point scale	+					-								-	+	+	+																
Hamano	2010	DM1	13	upper leg, lower leg	6 grades	+	-	+	+		-			+	+							+																
Kornblum	2006	DM2	14	whole-body	5 grades														-					-	+				++									
Stramare	2010	DM2	5	shoulder, pelvis, upper leg, lower leg	6 grades							+	+	+	+				+	+	+	+			+						+							
Degardin	2010	DM2	4	shoulder, pelvis, upper leg, lower leg	4 grades											-	-	-								-	-	-										

Figure 1: PRISMA flow diagram

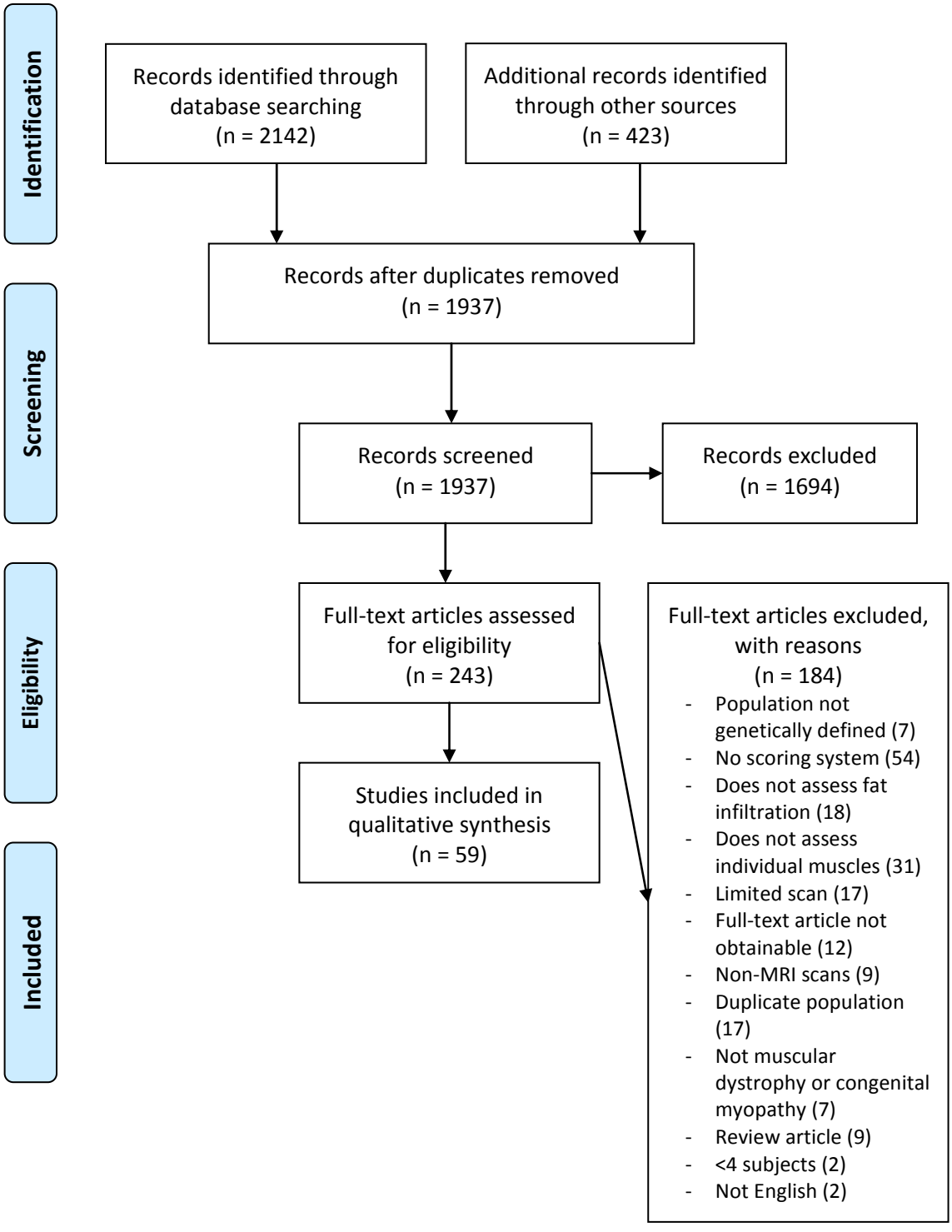

Figure 2: Example of sparing of the sartorius (arrow) and gracilis (arrowhead) in FSHD.

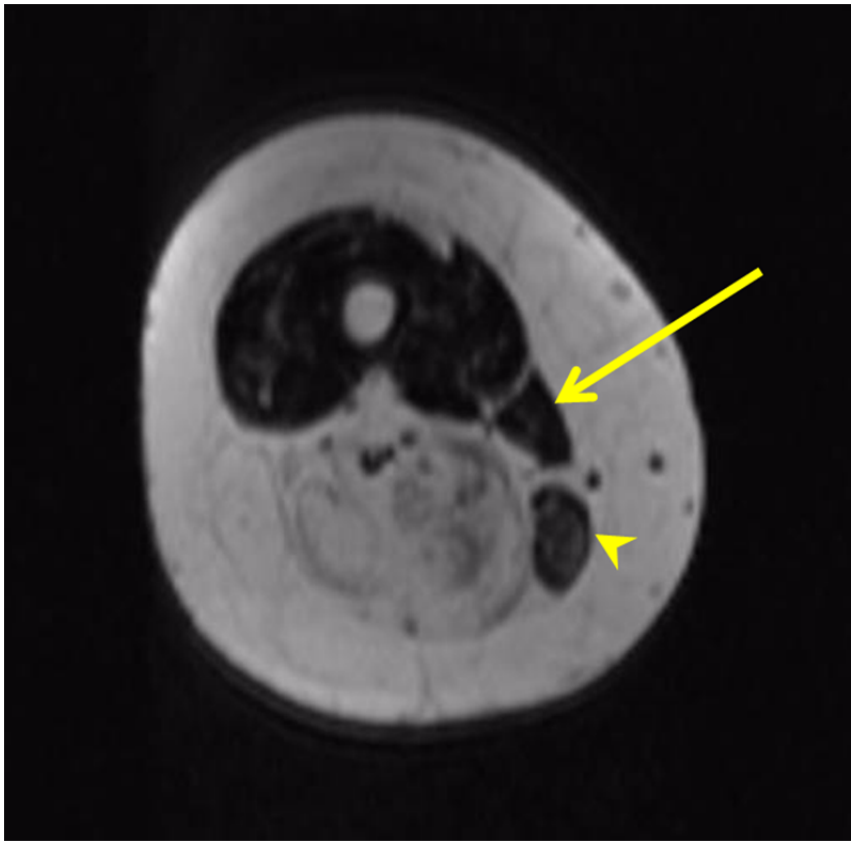

Chapter 2: Whole-body MRI in facioscapulohumeral muscular dystrophy

Abstract

Introduction: Facioscapulohumeral muscular dystrophy (FSHD) is a hereditary disorder that causes progressive muscle wasting. Growing knowledge of the pathophysiology of FSHD has stimulated interest in developing biomarkers of disease severity.

Methods: Whole-body MRI was used to scan 24 adults with genetically-confirmed type 1 FSHD. Muscles were scored for fat infiltration and edema-like changes. Fat infiltration scores were compared to muscle strength and function measurements.

Results: Our analysis reveals a distinctive pattern of muscle involvement and sparing in FSHD. Averaged fat infiltration scores for muscle groups in the legs were statistically significantly associated with quantitative muscle strength and 10-meter walk times.

Discussion: Advances in MRI technology allow for the acquisition of rapid whole-body imaging in diffuse muscle disease. This technique offers a promising disease biomarker in FSHD and other muscular dystrophies.

Background

Facioscapulohumeral muscular dystrophy (FSHD) is an autosomal dominant muscle disease with an estimated prevalence of 3.96 per 100,000, making it one of the most prevalent forms of muscular dystrophy.[1] Even before the genetic mutations associated with FSHD were identified, FSHD was considered a unique form of muscular dystrophy due to its characteristic pattern of muscle weakness that preferentially affects the face, arms, and shoulder girdle. The phenotypic spectrum of FSHD varies widely, with some individuals presenting in infancy with severe weakness and others remaining asymptomatic until the 7th decade of life.

In the past ten years, there has been great progress in elucidating the genetic and epigenetic mechanisms of disease in FSHD. More than 95% of affected individuals have a deletion in the long arm of chromosome 4, but more recently, mutations in the SMCHD1 gene on chromosome 18 have also been found to produce the same pattern of weakness.[2] The common mechanism of disease for both mutations is the hypomethylation of the 4q region. This region contains a series of 3.3 kilobase repeats (D4Z4 repeats), and hypomethylation of this region is believed to lead to multiple disease-related downstream effects.[3] Each D4Z4 repeat contains a copy of DUX4, a gene that is expressed during development, but later chronically suppressed.[4] Several groups of investigators have identified increased expression of DUX4 in muscle from individuals with FSHD, and overexpression of DUX4 in animal models has been shown to cause muscle toxicity.[5,6]

Our increased understanding of the pathophysiology of FSHD has produced several promising treatment targets. However, the ability to translate basic scientific discoveries into treatment is limited in part by the absence of appropriate biomarkers of muscle disease.[7] The need for biomarkers is particularly relevant in FSHD, which can be very slowly progressive with long periods of clinical stability. Clinical changes may occur over the course of years in FSHD, which increases the difficulty of performing clinical trials in this patient population.[8] A radiological biomarker that is both noninvasive and sensitive to changing severity in a slowly progressive disorder like FSHD could not only improve our understanding of the disease and its progression, but also facilitate quicker clinical trials.

Magnetic resonance imaging (MRI) is increasingly being recognized as a diagnostic and monitoring tool in skeletal muscle disease due to its ability to measure soft tissue characteristics.[9,10] Although morphologic MRI has been used as an outcome measure in clinical research involving myopathy, scans are often limited anatomically

(for instance, to the lower extremities) due to time constraints.[11,12] The development of whole-body MRI (WBMRI) scanning technology overcomes this limitation by allowing investigators to scan multiple regions in the body in a clinically feasible time (typically 1 hour or less).

WBMRI may be particularly useful in the detection and characterization of skeletal muscle pathology in FSHD. Studies using localized MRI in FSHD suggest that extensive subclinical disease can precede clinically detectable muscle weakness.[13,14] T1-weighted imaging has been used to identify the degree of muscle replacement by fat, and hyperintensity on fluid-sensitive sequences has been shown to correspond to an active inflammatory phase that precedes fat infiltration in FSHD.[15-17] Muscle involvement in FSHD can be asymmetrically distributed over multiple regions of the body, however, and the use of localized scanning in these studies does not allow for the examination of the temporal patterns of muscle involvement across different regions.[18]

In order to evaluate the feasibility of performing whole-body MRI in FSHD, we performed a cross-sectional study of adults with a wide spectrum of disease severity. The resultant images were used to provide descriptive data on the pattern of muscle involvement in FSHD and to analyze the associations between clinical and imaging measurements.

Methods

Study design and setting

The study protocol was approved by the Johns Hopkins School of Medicine Institutional Review Board. Adults with FSHD were invited to participate in a single-center, cross-sectional study. Participation consisted of an outpatient clinic visit and MRI scan. The clinic visits were conducted at the Kennedy Krieger Outpatient Clinic, and MRI

scans were performed at the Johns Hopkins Hospital (both facilities are located in Baltimore, Maryland).

Recruitment of study participants

Study participants were recruited through IRB-approved announcements in the newsletter of the FSH Society, Inc., through the clinicaltrials.gov registry (NCT01671865), and from the clinic population of the Center for Genetic Muscle Disorders at the Kennedy Krieger Institute. Written informed consent was obtained from each participant prior to enrollment. All participants had previously undergone genetic testing to detect the deletion in chromosome 4 associated with type 1 FSHD. Participants whose genetic testing predated routine testing for the 4qA haplotype were not asked to undergo repeat testing if they had a clinical presentation consistent with FSHD. However, participants who were asymptomatic had confirmatory 4qA haplotype testing. Other inclusion criteria included: age ≥18 years, ability to ambulate independently, and ability and willingness to give informed consent. Exclusion criteria included standard contraindications to MRI scanning. Participants who had undergone scapular fixation were also excluded, as wires and other implants could create field distortions and artifacts in regions of interest despite being MRI-safe. Contraindications to MRI were ascertained through screening forms and in-person screening assessments performed by radiology personnel immediately prior to scanning.

Clinical data collection

Each enrolled participant was examined by the author prior to MRI. Demographic data (age, gender, race/ethnicity) and results of genetic testing for FSHD were documented. Manual muscle testing (MMT) using the Medical Research Council (MRC) scale was performed for each participant. Quantitative muscle testing (QMT) was

performed using a hand-held dynamometer (Chatillon DPP series mechanical force gauge). The maximum voluntary isometric force of shoulder abduction, elbow extension, elbow flexion, hip flexion, knee extension, and knee flexion from the better of 2 trials was recorded for each participant.[19] A 10-meter timed walk was also performed for each participant.

MRI protocol

Magnetic resonance images were acquired using a 3 Tesla Magnetom Tim Trio system (Siemens, Erlangen, Germany) with continuous table movement (CTM). Participants were placed in a head-first, supine position, and all images were acquired with the participant in this fixed position. Five radiofrequency coils were placed on the participant: an 8-channel head coil, a neck matrix coil, 2 body matrix coils (1 for the chest and 1 for the abdomen/pelvis) and a peripheral angiography (PA) matrix coil positioned over the legs. Fat-suppressed T1-weighted [repetition time (TR)/echo time (TE)=150/3.69ms, field of view (FOV)=50x50cm^2, matrix size=320x161, inversion time (TI)=220ms, slice thickness=5mm, acquisition time 3:09 minutes] and Short Tau Inversion Recovery (STIR) (TR/TE=1200/86ms, FOV=50x50cm^2, matrix size=256x256, TI=240ms, slice thickness = 4-6mm, acquisition time 4:10 minutes) images were acquired using newly-developed CTM sequences. Both sequences scanned a total length of 1590mm (Figure 1). Images from the thorax and abdomen were acquired during 12-15 second breath-holds to minimize artifact from diaphragmatic movement.

Imaging outcomes

Skeletal muscle characteristics for all study participants were scored by a single reviewer. All muscles visualized on T1-weighted images were scored for the degree of intramuscular infiltration and replacement. Histopathologic studies of FSHD and other

muscular dystrophies suggest that these infiltrates are composed primarily of fat, although regions of perimysial and endomysial fibrosis are interspersed among (and radiographically indistinguishable from) the fatty tissue.[20,21] The scoring scale used to assess fat infiltration was previously described by Mercuri et al. (examples of scored muscles are shown in Figure 2).[22] A minor modification was made to the fat infiltration scale; an additional score level of 5 was added to signify 100% fat infiltration on T1-weighted imaging. This new score level was felt to be biologically significant as it would define a stage of disease at which no further fat infiltration could occur. For each muscle, the frequency of involvement, the mean fat infiltration score, and the frequency of asymmetric involvement across the study sample were calculated. Each of the muscles scored on T1-weighted imaging was classified as either involved/affected (score 2 or higher) or spared (score 0 or 1). Muscle pairs were defined as asymmetric if there was any difference in fat infiltration score between the right and left muscles in a single individual. Muscles were ranked by frequency of involvement, the mean fat infiltration scores, and the proportion of asymmetric muscle pairs. Muscles visualized on STIR images were scored on a dichotomous scale, with hyperintensity being either present or absent.

Data analysis

Exploratory graphs, pairwise correlation tests, and linear regression models were used to study the associations between clinical outcomes and fat infiltration scores on MRI. Scores for individual muscles comprising the hip flexors (iliopsoas, iliacus, psoas major), quadriceps (vastus lateralis, vastus medialis, vastus intermedius, rectus femoris), hamstrings (semitendinosus, semimembranosus, long and short heads of the biceps femoris), biceps brachii (long and short heads), triceps (long, lateral, and medial heads), deltoids (anterior, medial, and posterior), and paraspinal muscles (lateral thoracic,

medial thoracic, lateral lumbar, medial lumbar) were averaged to produce a mean fat infiltration score for each muscle group, which was analyzed as the predictor variable. The muscle strength (in pounds) was regressed against the mean fat infiltration scores for different muscles groups using univariable regression analyses that allowed for clustering within individual participants (to account for possible correlation between the right and left legs). Univariable and multivariable linear regression models were used to evaluate the associations between 10-meter walk times and mean MRI scores in the hamstrings, hip flexors, quadriceps, paraspinal, and abdominal muscles (these muscle groups were selected because they were scanned in their entirety in all participants). All analyses were performed using the Stata 12/IC statistical software package (StataCorp LP, College Station, Texas). Figures were created using both Stata 12/IC and R version 3.1.0.

Results

Study participants

Twenty-four participants (11 male, 13 female) met all screening criteria and were enrolled in the study (Table 1). The majority of participants (16 of 24) were recruited through advertising efforts; of these 16 participants, 13 were recruited through patient advocacy publications (both in print and online) and 3 cited the listing for this study in clinicaltrials.gov. Six participants were recruited from the clinic population at our center, and two were referred by other participants. All participants were enrolled and scanned between June 1, 2013 and November 30, 2014. The mean age of the study population was 52.5 years (standard deviation 12.3, range 20 to 72). All participants completed the study in its entirety and no complications were reported. For each participant, 89 to 118 muscles were visible and scored for fat infiltration and edema-like abnormalities.

Frequency, severity, and distribution of muscle involvement

There was considerable variability in disease severity between participants, and this is reflected in the percentage of muscles that were affected within these individuals. Between 1.7% and 78.6% of muscles were affected in individual participants. Asymmetric muscle involvement was also common; over the study sample, 294 of 1327 muscle pairs (22.2%) that were affected (either unilaterally or bilaterally) were asymmetrically affected. Table 2 lists the frequency, severity, and asymmetry of fat infiltration for each of the muscles that were scored. The most frequently and severely involved muscle was the semimembranosus (79% of the muscles visualized were affected and the mean fat infiltration score was 3.35). This is consistent with previously reported data using localized MRI of the lower extremities in FSHD.[23] Muscles of the trunk (paraspinal and abdominal wall muscles) were also among the most frequently affected (Figure 3).

Examination of the frequency of muscle involvement also identified several muscles that were unaffected across the study sample. These include the supraspinatus, infraspinatus, subscapularis, teres minor, and coracobrachialis muscle in the upper extremity, and the obturator internus and obturator externus in the pelvis. Preferential muscle involvement and sparing is illustrated in the heat map (Figure 4), which depicts fat infiltration scores across the study sample.

STIR imaging analysis

Only a minority of muscles in each participant were hyperintense on STIR imaging. Over the entire study sample, only 167 muscles out of the 2654 scored (6.3%) were judged to be hyperintense. However, only two of the 24 participants in the study did not have any STIR hyperintense muscles. In the other 22 participants, between 0.8% and 15.1% of muscles were characterized as STIR hyperintense. The most frequently

hyperintense muscle was the tibialis anterior (42.9% hyperintense), followed by the vastus medialis (29.2%) and medial gastrocnemius (26.1%). Although STIR hyperintensity was found in muscles at all levels of fat infiltration, it was most commonly observed in muscles with intermediate levels of fat infiltration (scores of 2 or 3) and rarely seen in muscles with the lowest or highest fat infiltration scores (Table 3).

Associations between MRI scoring and strength/function measurements

Figure 5 shows quantitative muscle strength (in pounds) for six muscle groups (hamstrings, quadriceps, hip flexors, deltoid, triceps, biceps) plotted against mean fat infiltration scores for these respective muscle groups. As these muscles were measured on both sides, each participant contributed two data points to each graph (signified by color). For the upper extremity muscle groups and the hip flexors, there were few individuals with MRI fat infiltration scores in the more severe ranges (the hip flexor groups, in particular, lacked data in the severely affected range). For these muscle groups, stable estimates of the association between fat infiltration scores and strength could not be obtained. The muscle group with the widest distribution of scores was the hamstrings. In this group, muscle strength appears to be relatively well-preserved (>40lbs) for mean fat infiltration scores <2. As mean fat infiltration scores increase beyond 2, the strength of the corresponding muscle group declines rapidly. Within this range, each one-point increase in the mean fat infiltration score was associated with a 10.9lb decline in knee flexion strength ($p=0.001$).

Examination of 10-meter walk times plotted against fat infiltration scores show a weak to moderate linear correlation for most muscle groups (Figure 6). A stronger linear correlation was demonstrated when fat infiltration scores for all of the lower extremity muscles were averaged and treated as a single muscle group ($r=0.75$, $p<0.0001$). Because the univariable regression models did not control for multiple comparisons, we

also used a multivariable regression model that included all muscle groups of the lower extremity and trunk (quadriceps, hamstring, hip flexors, paraspinal, and abdominal muscles) as predictors. The multivariable regression model showed a statistically significant association between the 10-meter walk time and fat infiltration scores in both the hip flexors and hamstrings. In this model, each one-point increase in mean fat infiltration score in the hip flexor group was associated with a 2.4 second increase in the 10-meter walk time ($p=0.003$). Each one-point increase in mean fat infiltration score in the hamstrings was associated with a 0.8 second increase in the 10-meter walk time ($p=0.029$).

Analysis of asymptomatic participants

Five of the study participants were described as having “non-manifesting” FSHD. These participants did not report any signs of weakness consistent with FSHD, but had been found to have the genetic mutation associated with FSHD after a family member presented with symptoms and was diagnosed. Examination of these participants showed normal strength testing. However, only one of these participants was found to have no affected muscles on MRI. The other participants were found to have fat infiltration in the muscles of the trunk and leg at varying levels of severity (Figure 7). All five of the non-manifesting participants had near complete sparing of the shoulder girdle muscles while all of the symptomatic individuals had severe involvement of at least one shoulder girdle muscle.

Discussion

In this study, we demonstrate the utility of WBMRI in examining global muscle involvement in muscular dystrophy. The use of whole-body imaging in this sample provides valuable new information on the distribution of disease by allowing us to

evaluate anatomic regions that are commonly affected in FSHD – such as the shoulder girdle and the trunk – but are rarely imaged in their entirety and cannot be tested individually using manual or quantitative muscle strength testing. The wide spectrum of disease severity captured using WBMRI in this study illustrates the heterogeneity of muscle involvement in FSHD that is only partially captured by existing disease biomarkers.

One of the salient findings of this study is that WBMRI can detect muscle involvement before loss of strength is discernible on physical examination. In our study sample, we were able to detect extensive fat infiltration of muscles in participants who had positive genetic testing but were asymptomatic. These findings would not have been detectable without the use of WBMRI. As increasing numbers of mildly affected, pre-symptomatic, or even non-manifesting patients are identified through genetic testing, MRI may allow clinicians to more accurately characterize their disease.

Our study also provides new data regarding the distribution of muscle involvement in FSHD. Severe weakness of some muscles and sparing of others is frequently observed in FSHD.[23,24] Whole-body imaging in our study sample expands upon this observation by identifying severely affected muscles (such as the paraspinal muscles) that cannot be easily examined in a clinical setting. Improved characterization of muscles that are preferentially affected may prove useful in elucidating the pathophysiology that produces the unique clinical findings in FSHD. Distinctive patterns of muscle involvement have been described in imaging studies of other muscular dystrophies and inflammatory muscle disorders, and the detailed characterization of these patterns could serve as a diagnostic tool in the evaluation of these disorders.[25,26]

The pattern of muscle involvement and sparing that we observe using WBMRI also provides indirect information about the natural history of FSHD. Although the order of muscle involvement cannot be definitively determined in a cross-sectional study, we

could reasonably assume that muscles that are most frequently affected across the study sample are affected earlier in the disease process. The frequent involvement of the hamstring muscles, for instance, suggests that they are among the earliest muscles affected in FSHD, but the experience of our center is that knee flexion weakness is rarely an early clinical complaint. This is likely due to sparing of the remaining muscles in that muscle group. The results of our study also suggest that progression of fat infiltration to the remaining hamstring muscles is associated with decline in muscle strength. A non-invasive predictor of clinical change would be a valuable tool for monitoring the progression of FSHD, and the ability to obtain a global view of all the muscle groups in one setting would help us understand the relationship between the clinical and subclinical manifestations of the disease.

Prior studies have indicated that there is an active phase of inflammatory muscle disease characterized by edema-like changes on fluid-sensitive MRI sequences (e.g. STIR), and that this phase is followed by rapid fat replacement.[15,17] Indirect evidence for this phenomenon comes from the distribution of fat infiltration scores in this and other studies.[27] Larger proportions of muscles were either severely affected or unaffected, while a relative minority of muscles fell in the intermediate levels (between 30-60%) of fat replacement (Table 3). This distribution suggests that the intermediate phase of muscle replacement occurs rapidly in FSHD, and the limited longitudinal data available in FSHD provides further support for this idea.[17, 27] Longitudinal WBMRI studies will therefore be an important next step in capturing the distribution of disease over time in this disease population.

There are some notable limitations to this study. Sample size is one of the most significant, particularly in a disease with high inter-individual variability. We anticipate that the small sample sizes are the primary reason for the lack of statistically significant associations between the 10-meter walk times and fat infiltration scores in the

quadriceps and hip flexors, as these muscles are likely to be major determinants of walking speed. Studies in larger numbers of patients will therefore be crucial in validating imaging biomarkers for use in clinical trials. We also excluded non-ambulatory patients and patients who had scapular fixation surgery. Both groups represent more severe phenotypes of FSHD and could be included in future studies. The whole-body imaging technique that we used also placed the arms near the edges of the magnet bore, resulting in distortional artifacts in these regions in a large proportion of participants.

Another limitation of this study is the use of fat-suppressed T1-weighted imaging to score fat infiltration. Prior studies that have scored fat infiltration in muscle have used non-fat suppressed images, which offer greater contrast between fat and muscle.[13] Non-uniformity of fat suppression during scanning also may affect the appearance of muscles and alter scoring results. Within our study sample, only fat-suppressed T1 sequences were obtained in all 24 participants with sufficient image quality for scoring. Qualitative comparisons of the fat-suppressed and the non-fat suppressed images (when available) increase our confidence that the fat-suppressed T1 sequences used in this analysis contain sufficient uniformity of fat suppression and contrast for semi-quantitative scoring. Nonetheless, these technical differences may limit the comparability of this study and other imaging studies in FSHD.

Another limitation to this study is the use of a semi-quantitative scoring method. Although this method is used frequently in MRI studies, the potential for inter-interpreter variability and bias is inherent to this type of rating scale. Another disadvantage to this method is the stratification of a continuous parameter (muscle infiltration) into only six levels of disease, which limits our ability to examine the association between muscle strength and fat infiltration within strata. Increasing evidence supports of the use of fully-quantitative imaging techniques and algorithms (such as Dixon imaging) to quantify fat replacement in skeletal muscle.[28] The incorporation of these quantitative measures into

whole-body MRI protocols would be an important next step in developing radiological biomarkers for FSHD and other generalized muscle diseases.

Despite these limitations, the wealth of information obtained using a WBMRI approach to FSHD promises new insight into the natural history of FSHD. Advanced MRI techniques and technology also provide the opportunity for rapid, standardized acquisition of high-quality images and a platform for the inclusion of novel imaging sequences in future studies of muscle disease.

References

1. Mah JK, Korngut L, Fiest KM, et al. A Systematic Review and Meta-analysis on the Epidemiology of the Muscular Dystrophies. The Canadian journal of neurological sciences Le journal canadien des sciences neurologiques 2016;43:163-77.

2. Lemmers RJ, Tawil R, Petek LM, et al. Digenic inheritance of an SMCHD1 mutation and an FSHD-permissive D4Z4 allele causes facioscapulohumeral muscular dystrophy type 2. Nat Genet 2012;44:1370-4.

3. Calandra P, Cascino I, Lemmers RJ, et al. Allele-specific DNA hypomethylation characterises FSHD1 and FSHD2. Journal of medical genetics 2016;53:348-55.

4. Snider L, Geng LN, Lemmers RJ, et al. Facioscapulohumeral dystrophy: incomplete suppression of a retrotransposed gene. PLoS Genet 2010;6:e1001181.

5. Rickard AM, Petek LM, Miller DG. Endogenous DUX4 expression in FSHD myotubes is sufficient to cause cell death and disrupts RNA splicing and cell migration pathways. Human molecular genetics 2015;24:5901-14.

6. Dandapat A, Bosnakovski D, Hartweck LM, et al. Dominant lethal pathologies in male mice engineered to contain an X-linked DUX4 transgene. Cell Rep 2014;8:1484-96.

7. Tawil R, Padberg GW, Shaw DW, van der Maarel SM, Tapscott SJ, Participants FW. Clinical trial preparedness in facioscapulohumeral muscular dystrophy: Clinical, tissue, and imaging outcome measures 29-30 May 2015, Rochester, New York. Neuromuscular disorders : NMD 2016;26:181-6.

8. A prospective, quantitative study of the natural history of facioscapulohumeral muscular dystrophy (FSHD): implications for therapeutic trials. The FSH-DY Group. Neurology 1997;48:38-46.

9. Del Grande F, Carrino JA, Del Grande M, Mammen AL, Christopher Stine L. Magnetic resonance imaging of inflammatory myopathies. Topics in magnetic resonance imaging : TMRI 2011;22:39-43.

10. Wattjes MP, Kley RA, Fischer D. Neuromuscular imaging in inherited muscle diseases. European radiology 2010;20:2447-60.

11. Wagner KR, Fleckenstein JL, Amato AA, et al. A phase I/IItrial of MYO-029 in adult subjects with muscular dystrophy. Annals of neurology 2008;63:561-71.

12. Forbes SC, Willcocks RJ, Triplett WT, et al. Magnetic resonance imaging and spectroscopy assessment of lower extremity skeletal muscles in boys with Duchenne muscular dystrophy: a multicenter cross sectional study. PloS one 2014;9:e106435.

13. Friedman SD, Poliachik SL, Carter GT, Budech CB, Bird TD, Shaw DW. The magnetic resonance imaging spectrum of facioscapulohumeral muscular dystrophy. Muscle & nerve 2012;45:500-6.

14. Olsen DB, Gideon P, Jeppesen TD, Vissing J. Leg muscle involvement in facioscapulohumeral muscular dystrophy assessed by MRI. Journal of neurology 2006;253:1437-41.

15. Tasca G, Pescatori M, Monforte M, et al. Different molecular signatures in magnetic resonance imaging-staged facioscapulohumeral muscular dystrophy muscles. PloS one 2012;7:e38779.

16. Kan HE, Scheenen TW, Wohlgemuth M, et al. Quantitative MR imaging of individual muscle involvement in facioscapulohumeral muscular dystrophy. Neuromuscular disorders : NMD 2009;19:357-62.

17. Friedman SD, Poliachik SL, Otto RK, et al. Longitudinal features of STIR bright signal in FSHD. Muscle & nerve 2014;49:257-60.

18. Tawil R. Facioscapulohumeral muscular dystrophy. Neurotherapeutics 2008;5:601-6.

19. Personius KE, Pandya S, King WM, Tawil R, McDermott MP. Facioscapulohumeral dystrophy natural history study: standardization of testing procedures and reliability of measurements. The FSH DY Group. Physical therapy 1994;74:253-63.

20. Moyer AL, Wagner KR. Regeneration versus fibrosis in skeletal muscle. Current opinion in rheumatology 2011;23:568-73.

21. Lin MY, Nonaka I. Facioscapulohumeral muscular dystrophy: muscle fiber type analysis with particular reference to small angular fibers. Brain & development 1991;13:331-8.

22. Mercuri E, Pichiecchio A, Allsop J, Messina S, Pane M, Muntoni F. Muscle MRI in inherited neuromuscular disorders: past, present, and future. Journal of magnetic resonance imaging : JMRI 2007;25:433-40.

23. Tasca G, Monforte M, Ottaviani P, et al. Magnetic Resonance Imaging in a large cohort of facioscapulohumeral muscular dystrophy patients: pattern refinement and implications for clinical trials. Annals of neurology 2016.

24. Rijken NH, van der Kooi EL, Hendriks JC, et al. Skeletal muscle imaging in facioscapulohumeral muscular dystrophy, pattern and asymmetry of individual muscle involvement. Neuromuscular disorders : NMD 2014;24:1087-96.

25. Kesper K, Kornblum C, Reimann J, Lutterbey G, Schroder R, Wattjes MP. Pattern of skeletal muscle involvement in primary dysferlinopathies: a whole-body 3.0-T magnetic resonance imaging study. Acta neurologica Scandinavica 2009;120:111-8.

26. Kornblum C, Lutterbey G, Bogdanow M, et al. Distinct neuromuscular phenotypes in myotonic dystrophy types 1 and 2 : a whole body highfield MRI study. Journal of neurology 2006;253:753-61.

27. Janssen BH, Voet NB, Nabuurs CI, et al. Distinct disease phases in muscles of facioscapulohumeral dystrophy patients identified by MR detected fat infiltration. PloS one 2014;9:e85416.

28. Dahlqvist JR, Vissing CR, Thomsen C, Vissing J. Severe paraspinal muscle involvement in facioscapulohumeral muscular dystrophy. Neurology 2014;83:1178-83.

Table 1: Demographic characteristics of participants in whole-body MRI study

Number	24
Gender	11 male/13 female
Age	52.5 (SD 12.3, range 20-72) years
Weight	77.1 (SD 17.8, range 49.9-129.3) kg
Height	171.5 (SD 8.6, range 157.5-188) cm
Restriction fragment size	24.8 (SD 5.7, range 10-32) kilobases

Table 2: Frequency, severity, asymmetry, and STIR hyperintensity of individual muscles

Muscle	Number scored (out of 48)	Number affected	Percent affected	Mean score across study sample	Percent with asymmetric fat infiltration	Percent STIR hyperintense
Semimembranosus	48	38	79.2%	3.35	41.7%	18.8%
Lower Rectus Abdominis	42	31	73.8%	3.26	33.3%	0.0%
Upper Rectus Abdominis	40	29	72.5%	2.88	40.0%	0.0%
Thoracic Medial Paraspinal	48	34	70.8%	2.56	12.5%	4.2%
Lumbar Medial Paraspinal	48	33	68.8%	2.56	16.7%	12.5%
Thoracic Lateral Paraspinal	48	33	68.8%	2.69	16.7%	6.3%
Serratus Anterior	48	30	62.5%	2.63	25.0%	8.3%
Lumbar Lateral Paraspinal	48	29	60.4%	2.42	29.2%	6.3%
Gluteus Minimus	48	28	58.3%	2.46	33.3%	4.2%
Latissimus	46	26	56.5%	2.50	21.7%	4.3%
Adductor Longus	48	27	56.3%	2.02	54.2%	0.0%
Tensor Fascia Lata	48	26	54.2%	2.29	33.3%	0.0%
Trapezius	36	19	52.8%	2.50	5.6%	0.0%
Adductor Magnus	48	25	52.1%	1.94	37.5%	20.8%
Gluteus Medius	48	25	52.1%	1.67	54.2%	2.1%
Biceps Femoris, Short Head	48	23	47.9%	2.17	20.8%	0.0%
Pectoralis Major	46	22	47.8%	1.67	26.1%	13.0%
Semitendinosus	48	22	45.8%	1.90	29.2%	10.4%
Rectus Femoris	48	22	45.8%	1.73	33.3%	0.0%
Biceps Femoris, Long Head	48	21	43.8%	1.81	37.5%	22.9%
Teres Major	47	20	42.6%	1.51	34.0%	17.0%
Vastus Medialis	48	18	37.5%	1.29	41.7%	29.2%
Gracilis	48	18	37.5%	1.35	20.8%	4.2%
Adductor Brevis	48	17	35.4%	1.40	25.0%	0.0%
Medial Gastrocnemius	46	16	34.8%	1.39	26.1%	26.1%
Pectoralis Minor	46	16	34.8%	1.37	34.8%	0.0%
Tibialis Anterior	42	14	33.3%	1.31	33.3%	42.9%
Sartorius	48	16	33.3%	1.23	45.8%	2.1%
Rhomboid	46	14	30.4%	1.43	26.1%	8.7%
Vastus Intermedius	48	13	27.1%	1.02	25.0%	0.0%
Triceps Lateral	8	2	25.0%	1.25	0.0%	25.0%

Gluteus Maximus	48	12	25.0%	0.90	16.7%	14.6%
Triceps Medial	8	2	25.0%	1.25	0.0%	12.5%
Quadratus Femoris	48	12	25.0%	0.92	29.2%	0.0%
Biceps Brachii Long	36	8	22.2%	0.97	22.2%	11.1%
Biceps Brachii Short	36	8	22.2%	1.00	27.8%	5.6%
Extensor Digitorum Longus	38	8	21.1%	0.79	31.6%	0.0%
Triceps Long	25	5	20.0%	0.80	24.0%	20.0%
Vastus Lateralis	48	9	18.8%	0.75	16.7%	18.8%
Lateral Gastrocnemius	46	7	15.2%	0.80	4.3%	2.2%
Soleus	40	6	15.0%	0.88	5.0%	2.5%
Quadratus Lumborum	48	7	14.6%	0.83	20.8%	0.0%
Iliopsoas	48	7	14.6%	0.52	20.8%	0.0%
Piriformis	48	7	14.6%	0.65	16.7%	0.0%
Pectineus	48	4	8.3%	0.27	16.7%	4.2%
Deltoid Posterior	44	3	6.8%	0.34	13.6%	13.6%
Deltoid Anterior	44	3	6.8%	0.34	9.1%	4.5%
Popliteus	44	3	6.8%	0.23	9.1%	0.0%
Brachialis	30	2	6.7%	0.40	13.3%	0.0%
Tibialis Posterior	40	2	5.0%	0.33	15.0%	0.0%
Deltoid Medial	41	2	4.9%	0.32	24.4%	4.9%
Peroneus Longus	41	2	4.9%	0.39	24.4%	0.0%
Iliacus	48	2	4.2%	0.17	0.0%	0.0%
Psoas Major	48	1	2.1%	0.08	12.5%	0.0%
Supraspinatus	21	0	0.0%	0.00	0.0%	0.0%
Infraspinatus	47	0	0.0%	0.00	0.0%	0.0%
Subscapularis	47	0	0.0%	0.00	0.0%	0.0%
Teres Minor	47	0	0.0%	0.00	0.0%	0.0%
Coracobrachialis	46	0	0.0%	0.04	0.0%	0.0%
Obturator Internus	48	0	0.0%	0.02	4.2%	0.0%
Obturator Externus	48	0	0.0%	0.06	4.2%	0.0%

Table 3: Frequency of fat infiltration scores and STIR hyperintensity in participants with FSHD

Fat infiltration score	Degree of fat infiltration	Number of muscles on WBMRI (% of 2654 scored muscles)	Number of STIR hyperintense muscles (% of muscles with this fat infiltration score)
0	no fat infiltration	1517 (57.2%)	53 (3.5%)
1	trace fat infiltration	308 (11.6%)	23 (7.5%)
2	<30% replacement of muscle with fat	213 (8%)	30 (14.1%)
3	30 to <60% replacement of muscle with fat	88 (3.3%)	16 (18.2%)
4	60 to <100% replacement of muscle with fat	285 (10.7%)	34 (11.9%)
5	100% replacement of muscle with fat	243 (9.2%)	5 (2.1%)

Figure 1: Examples of T1-weighted and STIR whole-body MRI scans in axial and coronal planes

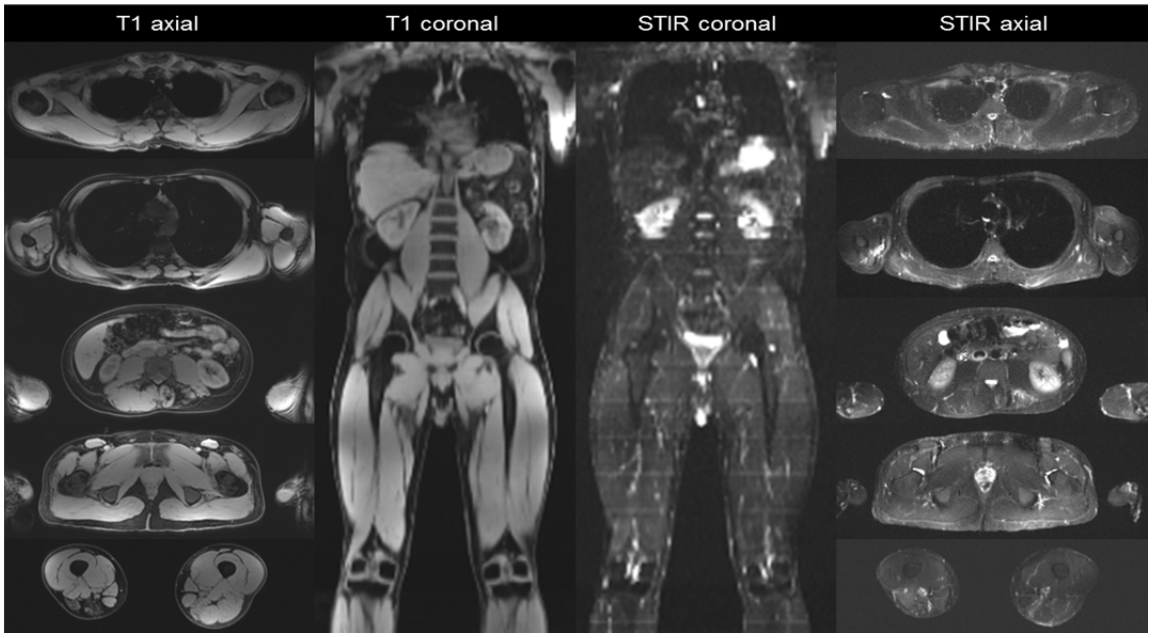

Figure 2: Representative axial T1-weighted images showing asymmetric fat infiltration in the bilateral thighs. In the rectus femoris, there is extensive fat replacement on the right (score 4), while the left side is unaffected (score 0). The bilateral adductor longus muscles are affected, with fat infiltration scores of 4 on the right and 5 (complete replacement) on the left. The semitendinosus muscles are less severely affected, with fat infiltration scores of 3 on the right and 2 on the left. Note that fat infiltration scores are assigned after visualization of the entire length of the muscle, not a single slice.

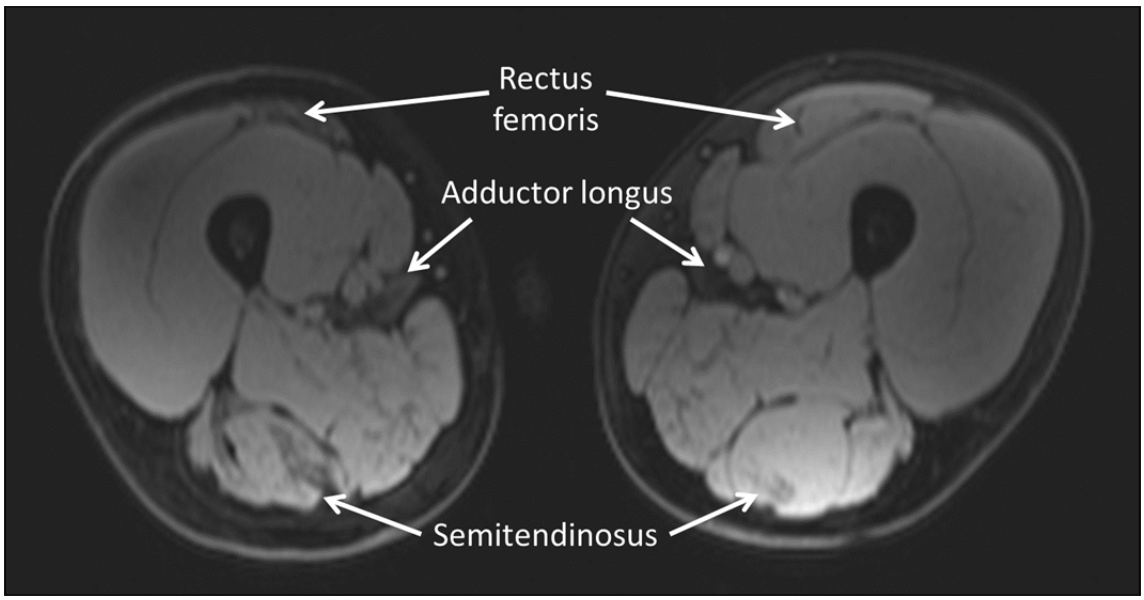

Figure 3: Examples of trunk muscle involvement in FSHD. Left column: T1-weighted (above) and STIR (below) images showing asymmetric fat infiltration and STIR hyperintensity in the left lumbosacral paraspinal muscles. Upper right: Asymmetric STIR hyperintensity of the left serratus anterior muscle. Lower right: T1-weighted imaging showing asymmetric atrophy of the right rectus abdominis muscles.

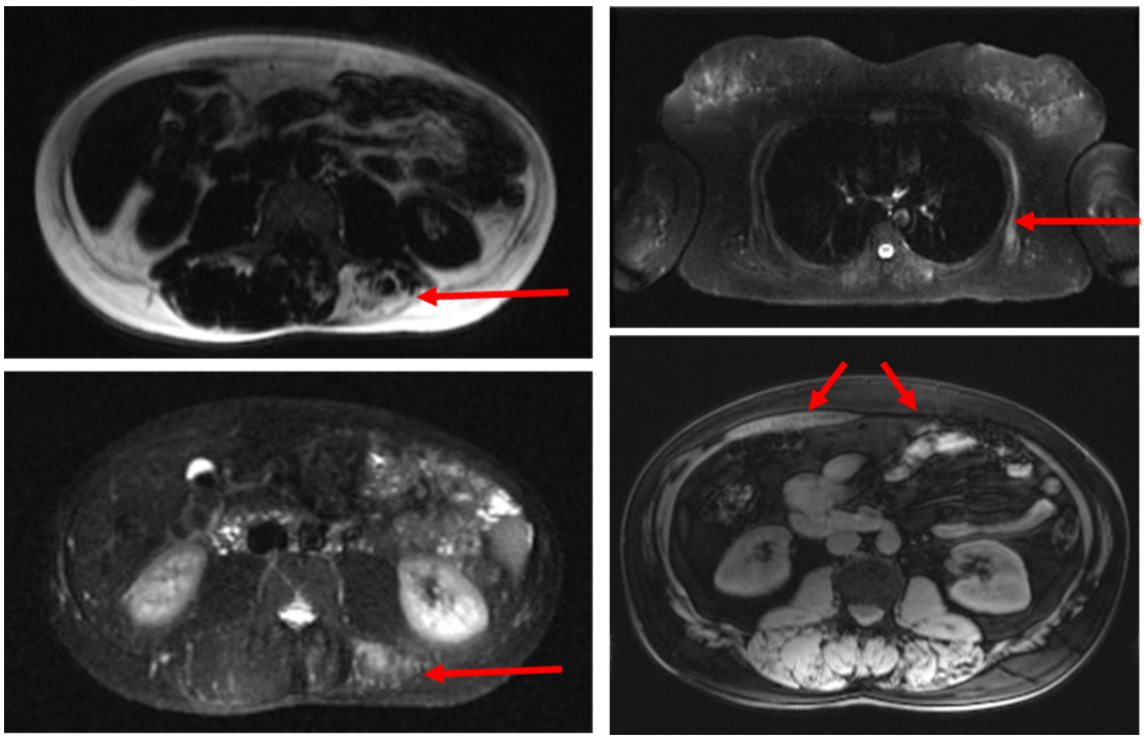

Figure 4: Heat map of fat infiltration scores in participants with FSHD. Participants are arranged (left to right) from lowest to highest mean MRI score (bottom row). Muscles on the left and right sides of the body are placed to the left and right sides (respectively) of the labeled tick marks for each participant. Fat infiltration scores on T1-weighted MRI (from 0 to 5) and their corresponding colors are shown in the numbered bar on the right.

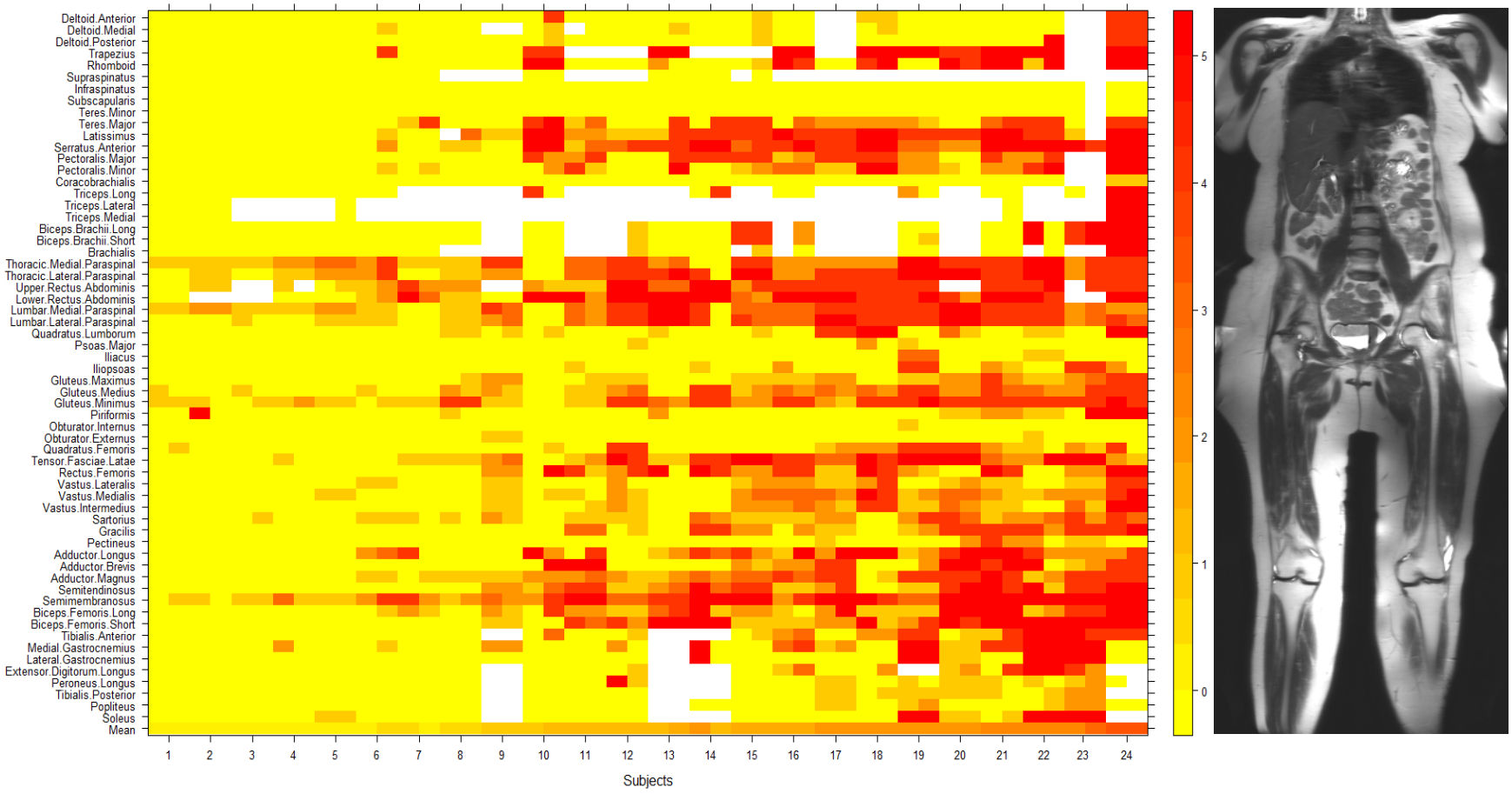

Figure 5: Fitted regression lines for muscle strength against mean fat infiltration MRI score in six muscle groups.

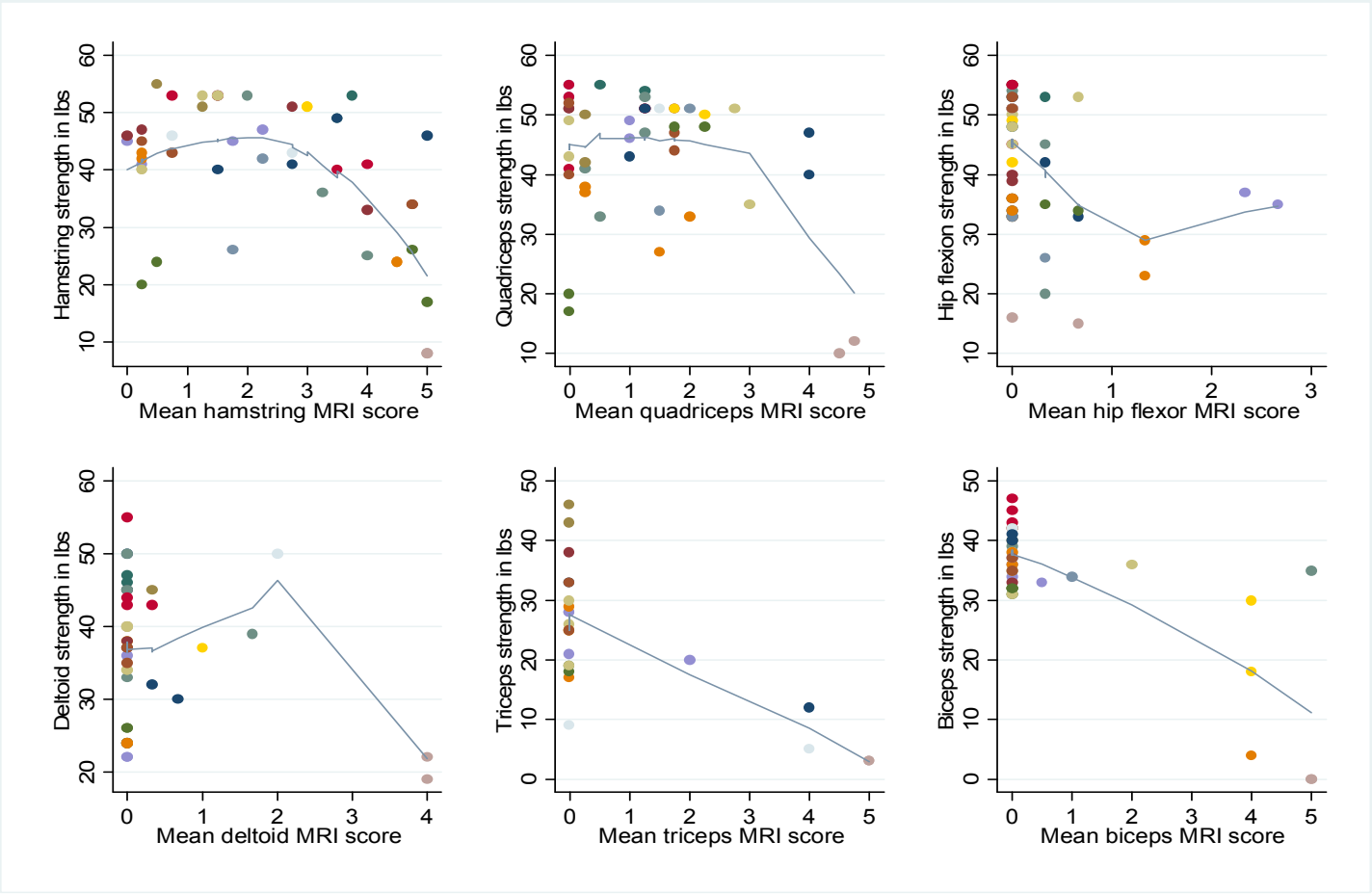

Figure 6: Fitted regression lines for 10-meter walk time against mean fat infiltration MRI score in five muscle groups and all leg muscles. Pearson correlation coefficients ("R") with their corresponding p-values are shown.

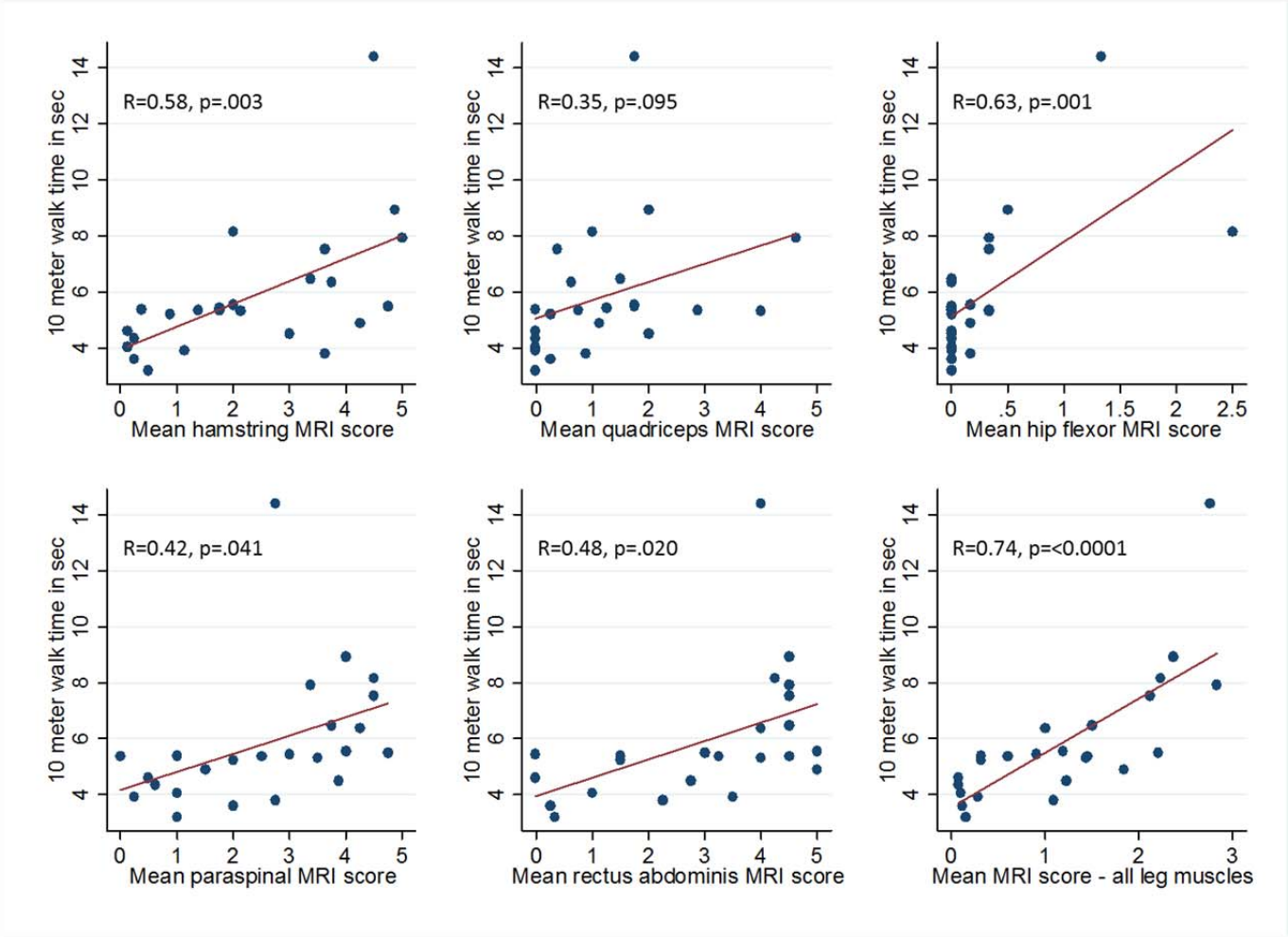

Figure 7: MRI of asymptomatic participants with FSHD confirmed by genetic testing. Left column: Fat-suppressed T1-weighted (above) and STIR (below) imaging of a 45-year-old male. Thigh imaging shows asymmetric fat infiltration (scored as 4 on the right, 2 on the left) of the semimembranosus muscles (arrows). There is a STIR hypointense area in the medial left thigh due to radiofrequency artifact from the MRI coil. Right column: Non-fat suppressed and STIR imaging of the pelvis of a 52-year-old female. The only abnormality seen on MRI was asymmetric absence of the left piriformis (arrows).

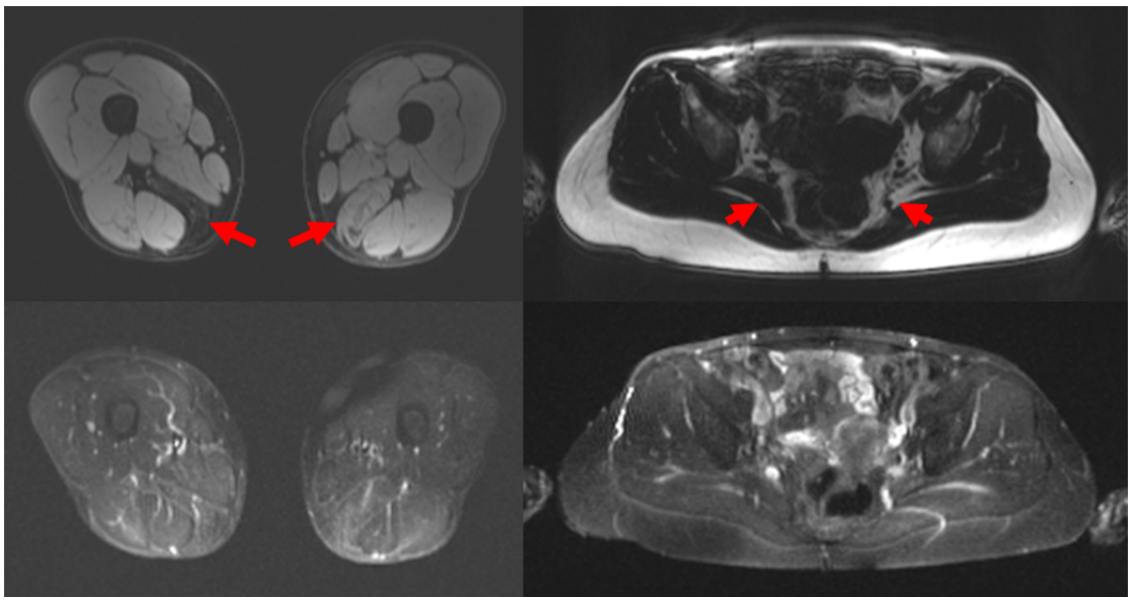

Chapter 3: An observational study of multivoxel proton magnetic resonance spectroscopy in facioscapulohumeral muscular dystrophy

Abstract

Introduction: Facioscapulohumeral muscular dystrophy (FSHD) is a hereditary disorder that causes progressive muscle wasting. Growing knowledge of the pathophysiology of FSHD has stimulated interest in developing quantitative biomarkers of disease severity that can be used in clinical trials and observational studies.

Methods: Thirty-six adults with FSHD and 15 healthy controls underwent multivoxel proton magnetic resonance spectroscopy (MRS) of an axial cross-section of the mid-thigh. The concentrations of creatine, intramyocellular lipids, extramyocellular lipids, and trimethylamine-containing (TMA) compounds in voxels corresponding to normal-appearing skeletal muscle were calculated. Metabolite concentrations for participants with FSHD were compared with those of controls. The associations between metabolite concentration and muscle strength were examined.

Results: Our analysis revealed a statistically significant reduction in the muscle TMA/creatine ratio in adults with FSHD compared to controls. The TMA/creatine ratio in the hamstrings also showed a moderate linear correlation with muscle strength.

Discussion: MRS offers a potential method of detecting muscle pathology in FSHD prior to the development of fat infiltration in these muscles. Further study is needed to determine the longitudinal pattern of these changes in the FSHD population.

Background

One of the earliest applications of magnetic resonance technology was magnetic resonance spectroscopy (MRS), a technique that distinguishes metabolites by their unique chemical shift properties when exposed to a magnetic field. Since the 1980s,

multiple investigators have used MRS to study phosphorus-containing (^{31}P) compounds in muscle.[1] Since ^{31}P is a component of ATP, phosphocreatine, and inorganic phosphate, ^{31}P MRS has been used in the study of energy consumption and exercise-related changes in muscle.[2,3]

Studies in mice and humans have identified metabolic profiles using ^{31}P MRS that are believed to be indicators of muscle degeneration and regeneration in Duchenne muscular dystrophy, and recent studies have reported similar findings in FSHD.[4-6] In 2010, Kan et al. showed that ^{31}P MRS was able to differentiate between fat infiltrated and unaffected muscles in individuals with FSHD and controls, providing further support for the use of MRS in monitoring disease progression.[7] More recently, Janssen et al. demonstrated that high-energy phosphate metabolite concentrations (specifically PCr/ATP) measured through MRS corresponded to the degree and rate of fat infiltration in specific muscles.[8]

Despite the established utility of phosphorus-based MRS in the study of muscle, the technique is not used routinely in clinical practice. This is due in part to the need for specialized hardware, software, and imaging expertise to adequately perform ^{31}P MRS studies. There has subsequently been interest in the development of proton (^{1}H) MRS in the study of skeletal muscle.[9-11] As all MRI scanners are programmed to collect information on proton-containing molecules, no additional hardware is required to perform proton MRS, and many MRI scanning systems now have built-in protocols that can be used to obtain spectroscopic data.

One of the technical challenges in performing proton spectroscopy in muscle has been the presence of large water and fat peaks that obscure smaller peaks corresponding to molecules of interest. Improvements in magnetic field homogeneity, gradients, and water suppression have now made it possible to use proton spectroscopy to reliably estimate the concentration of metabolites such as creatine and

trimethylamines (TMA) in muscle.[12] Proton MRS can also be used to distinguish the intramyocellular (IMCL) and extramyocellular (EMCL) lipid peaks within muscle.[13] As fat infiltration is a prominent pathological feature of the muscular dystrophies, this capability may be useful in characterizing pathology in these diseases.

Another improvement in MRS technique that may enhance its utility in the study of muscle tissue is the ability to acquire data from multiple voxels in a single acquisition. Routine single-voxel spectroscopy protocols share the same disadvantages as muscle biopsy in that they examine small regions of large muscles and can therefore miss areas of disease pathology. Performing MRS in multiple voxels previously required a greater number of phase encoding steps, which increased the scan time at a prohibitive rate. However, the development of various fast MRS techniques (such as multiple-echo acquisition, echo-planar spectroscopy imaging, and parallel encoded MRS) has reduced the scan time and allowed the efficient acquisition of spectra over large regions. These spectra can then be mapped onto anatomic images to better appreciate spatial variations in the metabolic profile over large regions of tissue.[14,15]

Studies of proton MRS in patients with inflammatory myopathy have shown that creatine concentrations are higher in patients with inflammatory myopathy compared to normal controls, even in muscle that appears normal on T1 and STIR (short-tau inversion recovery) MRI scans. These findings suggest that changes in MRS profiles may precede findings on traditional anatomic imaging.[16] If spectroscopy can be shown to reliably predict loss of muscle strength and function in muscular dystrophy, it could benefit the field of muscular dystrophy research in multiple ways. First, it would identify early stages of disease pathology that precede fat infiltration, which is believed to be an irreversible stage of disease. Second, the ability to detect or predict short-term changes in muscle pathology could facilitate clinical trials in this patient population by allowing for trials of shorter duration.

To determine if muscle metabolite concentrations differ in anatomically normal-appearing muscles in FSHD, we performed an observational cross-sectional study of multivoxel proton spectroscopy in adults with FSHD and unaffected healthy controls.

Methods

Study design and setting

The study protocol was reviewed and approved by the Johns Hopkins Institutional Review Board. Adults (older than 18 years) with genetically-confirmed FSHD and healthy volunteers were invited to participate in a single-center, cross-sectional study. All participants were asked to undergo confirmatory gene testing for type 1 FSHD if it had not been done prior to enrollment. Each potential participant was screened for contraindications to MRI scanning (such as implanted metal devices). Participants were asked to return for an optional second scan between 18 and 24 months following the initial scan.

Clinical data collection

Demographic information (age, gender, height, weight) was collected for each participant. Enrollees with FSHD were asked to provide copies of their genetic testing results. Healthy volunteers were asked to undergo genetic testing for FSHD to confirm the absence of disease. On the day of each scan, participants underwent strength testing of the hip flexors, knee flexors, and knee extensors using hand-held dynamometry. A 10-meter walk time was also measured.

MRI protocol

All scans were performed at the Johns Hopkins Hospital in Baltimore, Maryland. Each participant was scanned using a 3 Tesla Siemens Tim Trio scanning system

(Siemens, Erlangen, Germany). Each participant was scanned in a supine, feet-first position. Two body matrix coils were placed over the upper and lower thighs. Multivoxel MR spectroscopy was performed in a single 10-mm slice centered in the mid-thigh of each leg (Figure 1). Shimming and water suppression were optimized using automated manufacturer protocols. The scanning parameters for water suppressed images were: TR/TE 1800/135 ms; matrix size 16 × 16; slice thickness 10 mm; field of view 16 × 16 cm; data acquisition time 7:17 minutes per leg. The nominal voxel size was 1.0 mL. The echo signal was digitized with 512 data points and a spectral width of 2,000 Hz. Unsuppressed water images were acquired with a four-element body matrix receiver coil (TR/TE 1800/30ms; matrix size 16 × 16; slice thickness 10 mm; field of view 16 × 16 cm; data acquisition time 4:35 minutes per leg).

Raw spectroscopy data were exported from the scanning system as RDA files and processed using LCModel software. Water suppressed and unsuppressed spectra were used to calculate metabolite concentrations in Institutional Units (IU) and as ratios with respect to the creatine peak.[17]

Voxels were selected for further analysis using a 2-level screening process. T1-weighted images that were used to select regions for spectroscopy acquisition were examined to identify voxels that were completely enclosed within muscle. The spectra corresponding to these voxels were subsequently examined for spectral quality. Spectra were excluded if they contained excessive noise or did not demonstrate identifiable metabolic peaks. Spectra with insufficient water suppression or field homogeneity were also excluded.

Data analysis

The distribution of metabolite concentrations was explored and examined for outliers using histograms and box plots. Excessively right-skewed data were log-

transformed, and q-q plots were used to confirm the normal distribution of the resultant data points. Multilevel linear regression models were used to assess differences in metabolite concentrations between affected and unaffected participants. Random effects parameters were included in the models to account for clustering within individual subjects and individual muscles within subjects. Mean metabolite concentrations in specific muscle groups were also examined with respect to strength and 10-meter walk time.

For the subset of participants who returned for follow-up scans, the metabolite concentrations were examined using two methods. The mean concentration of each metabolite was calculated for each muscle. The difference in the mean metabolite concentration between the baseline and follow-up scans was analyzed using histograms, t-tests, and Bland-Altman plots. Multilevel linear regression models were also used to study the concentration of each metabolite studied with respect to time (also grouped by individual subject and muscle). Data analysis was performed using the Stata 12/IC statistical software package (StataCorp LP, College Station, Texas).

Results

Study participants

A total of 51 participants were included in the observational study (36 with FSHD and 15 healthy controls). All participants were enrolled and scanned between April 16, 2012 and January 30, 2015. The majority of enrollees with FSHD (25 of 36) responded to advertising through patient advocacy groups or clinicaltrials.gov. Of the remaining 11, nine were recruited from the clinic population at our center and two were referred by other participants. Throughout the screening process, only five potential participants who contacted the study team did not meet inclusion criteria for the study; four were excluded because they did not have confirmatory genetic testing for FSHD, and one had a

contraindication to MRI. Two people who did meet inclusion criteria ultimately did not participate; one canceled the visit due to scheduling conflicts, and another initially agreed to participate and later withdrew owing to claustrophobia.

Recruitment of controls was limited to volunteers that could be matched to affected participants by age and gender. As participants with FSHD were accrued, they were divided into groups of no more than three, with each group being of the same gender and within 5 years of age of each other. Controls were selected so that each group was matched to at least one unaffected participant of the same gender whose age was within three years of the mean age of the group members. Among the healthy controls enrolled, only one was recruited through advertising. Five controls were unaffected relatives of clinic patients or participants in other studies at our center. The remaining nine controls were recruited from among employees at our center.

Cross-sectional data comparing FSHD and controls

All participants with FSHD were found to have a causative deletion on chromosome 4. Fourteen of the healthy controls did not have a deletion, and the single control that was found to have a deletion did not have the 4qA haplotype that is required to develop FSHD.[18] The demographic features of the affected and unaffected participants are summarized in Table 1. Genetic testing results from participants with FSHD show a broad range of deletion sizes (restriction fragment sizes range from 10 to 33 kb).

Proton MRS was completed in both legs for most participants (3 participants had only one leg studied). Spectra were collected from 256 individual voxels in each leg. Screening for voxels that were completely enclosed within muscle excluded 78% of acquired voxels, and screening for spectral fit excluded an additional 13% of the acquired voxels. Preliminary examination of the fat and water spectroscopy imaging

indicated that there was insufficient field homogeneity in the majority of scans performed in the right lower extremity, and therefore only spectra from the left lower extremity were included in the analysis. The remaining 1165 voxels (representing 32 participants with FSHD and 14 controls) were included in the statistical analysis. No usable voxels were identified in 5 participants (4 affected and 1 control), and the remaining participants each contributed between 7 and 38 voxels to the data set. These voxels represent 12 individual muscles of the thigh.

The most commonly identified metabolite peaks included trimethylamines (TMA) at 3.2 ppm, creatine (Cr) at 3.0 ppm, an extramyocellular lipid (EMCL) peak at 1.5 ppm, and an intramyocellular lipid (IMCL) peak at 1.3 ppm (Figure 2). The concentrations of these metabolites with respect to water and creatine were selected for further analysis. Multilevel regression models were used to evaluate differences in metabolite concentration between affected and unaffected participants while accounting for grouping within muscles and individual participants. These analyses demonstrated a statistically significant difference in TMA/Cr between affected and unaffected participants ($p=0.001$) (Figure 3, Table 2). No statistically significant differences were identified in the concentrations of creatine, TMA, IMCL, and EMCL or the ratios of these metabolites with respect to creatine (Figure 4).

Comparison of metabolite concentration and clinical measurements in FSHD

The concentrations of creatine, TMA, IMCL, and EMCL of voxels located in the quadriceps (vastus lateralis, vastus medialis, vastus intermedius, and rectus femoris muscles) and hamstrings (semitendinosus, semimembranosus, long and short heads of the biceps femoris) were averaged for each participant with FSHD. These muscle group means were then plotted against strength in these respective muscle groups. Only TMA/Cr showed a moderate linear correlation with strength in the hamstrings, indicating

that muscle strength is greater in voxels with higher log[TMA/Cr] (r=0.62, p=0.0002). There was a weaker correlation between TMA/Cr concentration and the 10-meter walk time, but higher log[TMA/Cr] values were associated with a statistically significant decrease in the 10-meter walk time (r=-0.41, p=0.026) (Figure 5). No statistically significant association between strength or function and log[TMA/Cr] was seen in the quadriceps, possibly owing to a narrower range of strength measurements in this muscle group. No significant association with muscle strength was observed in any of the other metabolites studied.

Longitudinal data analysis

Longitudinal spectroscopy data was obtained from ten participants with FSHD. Acquisition and analysis of spectra was performed using the same protocol as the baseline scan. There were no statistically significant differences in knee flexion and knee extension strength between the baseline and 18-24 month follow-up scans. Multilevel regression models did not show any significant change in concentration from baseline to follow-up for any of the metabolites analyzed. Figure 6 shows boxplots for each metabolite. The difference in mean concentration between the baseline and follow-up studies for each muscle was not statistically significantly different from zero for any of the metabolites studied. Bland-Altman plots were also used to examine the distribution of the differences in metabolite concentration between the baseline and follow-up scans (Figure 7).

Discussion

We have demonstrated that in muscles that are normal-appearing on T1-weighted MRI, multiple metabolites can be quantified using multivoxel proton MRS. Comparing adults with FSHD to unaffected matched controls, there is a statistically

significant difference in the intramuscular TMA/Cr ratio. These findings are similar to prior studies by Hsieh et al., which also identified a decreased TMA/Cr ratio in patients with Duchenne muscular dystrophy compared to healthy controls.[11] These investigators also found statistically significant differences in the TMA/water and creatine/water ratios comparing affected and unaffected participants, but our analysis did not reproduce this finding in FSHD.

Examination of the TMA and Cr data suggest that the difference in TMA/Cr is primarily driven by the difference in TMA concentration, which is reduced in affected participants compared to controls. Although the TMA concentrations with respect to water did not differ significantly between affected and unaffected participants, this may be due to the variability in concentration found for this particular metabolite. In brain spectroscopy, the TMA peak is believed to contain signal from choline-containing compounds, including phospholipids that are implicated in cell membrane metabolism, and a reduced concentration of these compounds may reflect the disruption of muscle cell membranes that occurs in FSHD.[19] Studies of muscle have also demonstrated that the TMA peak is comprised of several different molecules involved in muscle metabolism, including carnitine and acetylcarnitine.[20] These compounds are involved in the transport of fatty acids across the mitochondrial membrane, and impairment in this process can result in metabolic myopathies. The relative reduction in TMA/Cr in affected muscle may reflect early muscle pathology that results in the loss of muscle membrane or mitochondrial components.

There are some limitations in this study. An examination of outliers demonstrated marked differences in metabolite concentrations in the postero-lateral aspect of the right lower extremity compared to the left. This may be related to a scanner-specific field defect. To compensate for this potential confounder, we analyzed only the left lower extremity for each participant, and this reduction in data may have reduced the power to

detect changes in metabolite concentrations. We also did not collect data on several factors that are known to influence the results of MRS, including exercise levels and medications. Spectroscopy can also be influenced by the T2 relaxation times of the tissue volumes that are being measured. Our protocol did not include T2-weighted imaging with slices that were co-registered with the T1-weighted images used to position the voxels, so there was no feasible method of controlling for this potential confounder.

Other potential limitations in this study relate to the post-processing steps. While it was anticipated that only a fraction of scanned voxels would be entirely enclosed within muscles, a large number of voxels were also excluded owing to poor spectral fit (Table 1). There are multiple reasons why this may have occurred, such as movement in the scanner. The number of voxels contributed by each participant also varied widely. Although our statistical model was adjusted to account for the effects of clustering, those participants who contributed more voxels to the dataset may still have a greater influence on the outcome of the analysis.

In the limited amount of longitudinal data that was collected, we did not clearly identify any statistically significant changes in metabolite concentration over time in this subset. This observation appears to conflict with prior data from studies of MRS in Duchenne muscular dystrophy that shows a time-dependent change in fat and water concentration.[21] However, this discrepancy may be related to the fact that only voxels corresponding to normal-appearing muscles on T1-weighted imaging were included in our analysis. Doing so would necessarily exclude voxels that had been replaced by fat between the baseline and follow-up scans. It is also possible that changes in spectroscopy are detectable over shorter periods of time in Duchenne muscular dystrophy because of the more rapid progression of disease. Further study is required to fully characterize the longitudinal changes in metabolite profiles in FSHD.

Our study demonstrates that the TMA/Cr ratio in skeletal muscle of adults with FSHD differs significantly from those of unaffected controls. This difference was found in normal-appearing muscle, suggesting that it is an early pathological change. There is also evidence that changes in the TMA/Cr ratio are associated with muscle strength. Further study is needed to determine the ways in which TMA/Cr levels change over time and whether or not these changes are predictive of deteriorating muscle function in FSHD.

References

1. Edwards RH, Dawson MJ, Wilkie DR, Gordon RE, Shaw D. Clinical use of nuclear magnetic resonance in the investigation of myopathy. Lancet (London, England) 1982;1:725-31.

2. Kemp GJ, Taylor DJ, Dunn JF, Frostick SP, Radda GK. Cellular energetics of dystrophic muscle. Journal of the neurological sciences 1993;116:201-6.

3. Barbiroli B, Funicello R, Ferlini A, Montagna P, Zaniol P. Muscle energy metabolism in female DMD/BMD carriers: a 31P-MR spectroscopy study. Muscle & nerve 1992;15:344-8.

4. Banerjee B, Sharma U, Balasubramanian K, Kalaivani M, Kalra V, Jagannathan NR. Effect of creatine monohydrate in improving cellular energetics and muscle strength in ambulatory Duchenne muscular dystrophy patients: a randomized, placebo-controlled 31P MRS study. Magn Reson Imaging 2010;28:698-707.

5. Heier CR, Guerron AD, Korotcov A, et al. Non-invasive MRI and spectroscopy of mdx mice reveal temporal changes in dystrophic muscle imaging and in energy deficits. PLoS ONE 2014;9:e112477.

6. Hogrel JY, Wary C, Moraux A, et al. Longitudinal functional and NMR assessment of upper limbs in Duchenne muscular dystrophy. Neurology 2016;86:1022-30.

7. Kan HE, Klomp DWJ, Wohlgemuth M, et al. Only fat infiltrated muscles in resting lower leg of FSHD patients show disturbed energy metabolism. NMR in biomedicine 2010;23:563-8.

8. Janssen BH, Voet NB, Nabuurs CI, et al. Distinct disease phases in muscles of facioscapulohumeral dystrophy patients identified by MR detected fat infiltration. PLoS ONE 2014;9:e85416.

9. Kim HK, Serai S, Lindquist D, et al. Quantitative Skeletal Muscle MRI: Part 2, MR Spectroscopy and T2 Relaxation Time Mapping-Comparison Between Boys With Duchenne Muscular Dystrophy and Healthy Boys. AJR Am J Roentgenol 2015;205:W216-23.

10. Willcocks RJ, Forbes SC, Finanger EL, et al. Magnetic resonance imaging and spectroscopy detect changes with age, corticosteroid treatment, and functional progression in DMD. Neuromuscular Disorders 2013;23:810.

11. Hsieh TJ, Jaw TS, Chuang HY, Jong YJ, Liu GC, Li CW. Muscle metabolism in Duchenne muscular dystrophy assessed by in vivo proton magnetic resonance spectroscopy. J Comput Assist Tomogr 2009;33:150-4.

12. Bongers H, Schick F, Skalej M, Jung WI, Stevens A. Localized in vivo 1H spectroscopy of human skeletal muscle: normal and pathologic findings. Magnetic resonance imaging 1992;10:957-64.

13. Boesch C, Decombaz J, Slotboom J, Kreis R. Observation of intramyocellular lipids by means of 1H magnetic resonance spectroscopy. Proc Nutr Soc 1999;58:841-50.

14. Fayad LM, Barker PB, Jacobs MA, et al. Characterization of musculoskeletal lesions on 3-T proton MR spectroscopy. AJR American journal of roentgenology 2007;188:1513-20.

15. Nelson SJ. Multivoxel magnetic resonance spectroscopy of brain tumors. Mol Cancer Ther 2003;2:497-507.

16. Subhawong TK, Wang X, Machado AJ, et al. 1H Magnetic resonance spectroscopy findings in idiopathic inflammatory myopathies at 3 T: feasibility and first results. Investigative radiology 2013;48:509-16.

17. Provencher SW. Automatic quantitation of localized in vivo 1H spectra with LCModel. NMR in biomedicine 2001;14:260-4.

18. Lemmers RJ, Wohlgemuth M, van der Gaag KJ, et al. Specific sequence variations within the 4q35 region are associated with facioscapulohumeral muscular dystrophy. American journal of human genetics 2007;81:884-94.

19. Deshmukh S, Subhawong T, Carrino JA, Fayad L. Role of MR spectroscopy in musculoskeletal imaging. The Indian journal of radiology & imaging 2014;24:210-6.

20. Ren J, Lakoski S, Haller RG, Sherry AD, Malloy CR. Dynamic monitoring of carnitine and acetylcarnitine in the trimethylamine signal after exercise in human skeletal muscle by 7T 1H-MRS. Magnetic resonance in medicine 2013;69:7-17.

21. Willcocks RJ, Rooney WD, Triplett WT, et al. Multicenter prospective longitudinal study of magnetic resonance biomarkers in a large duchenne muscular dystrophy cohort. Annals of neurology 2016;79:535-47.

Table 1: Demographic information and voxel characteristics.

	FSHD	Controls
Number	36	15
Gender	15 male/21 female	6 male/9 female
Age (years)	50 ± 13.6 [20-71]	51.5 ± 14.3 [23-70]
Weight (kg)	77.6 ± 17.9 [49.9-111.1]	77.0 ± 15.1 [59-106.6]
Height (cm)	170.2 ± 7.9 [157.5-188]	167.1 ± 9.9 [155-182.9]
Deletion (kb)	25.3 ± 5.3 [10-35]	77 ± 29.3 [12-130]
Number of voxels	17920	7424
Voxels enclosed	3967	2295
Good spectral fit	1665	847
Left side only	812	353

Table 2: Concentration of 7 metabolites in participants with FSHD and controls (represented as means and 95% confidence intervals). P-values were obtained through multilevel linear regression analyses.

Metabolite	FSHD	95% Confidence interval	Control	95% Confidence interval	p-value
Creatine	0.00145	0.00115, 0.00184	0.00153	0.00107, 0.00219	0.802
TMA	0.00027	0.00021, 0.00035	0.00042	0.00028, 0.00063	0.065
TMA/Cr	0.17652	0.15569, 0.20014	0.25895	0.21450, 0.31262	0.001
IMCL	0.01076	0.00813, 0.01425	0.01565	0.01027, 0.02385	0.147
IMCL/Cr	7.21004	5.20847, 9.98079	10.05499	6.16943, 16.38772	0.267
EMCL	0.06963	0.04990, 0.09718	0.05519	0.03341, 0.09116	0.449
EMCL/Cr	48.91152	41.12672, 58.16990	39.13538	30.13647, 50.82142	0.163

Figure 1: Representative multivoxel grids positioned over the mid-thigh in a healthy control (above) and a participant with FSHD (below).

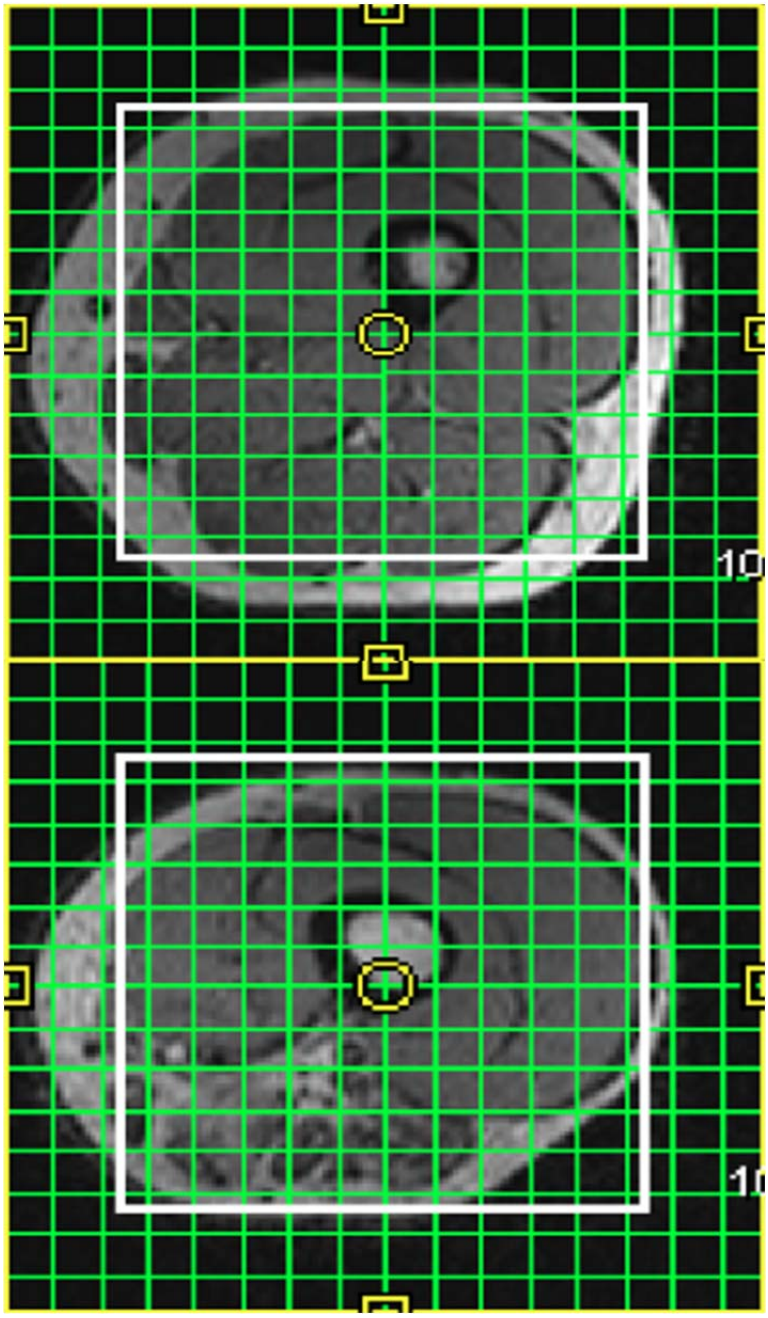

Figure 2: Representative spectra from a single voxel in a participant with FSHD. The peaks corresponding to the analyzed metabolites are labeled.

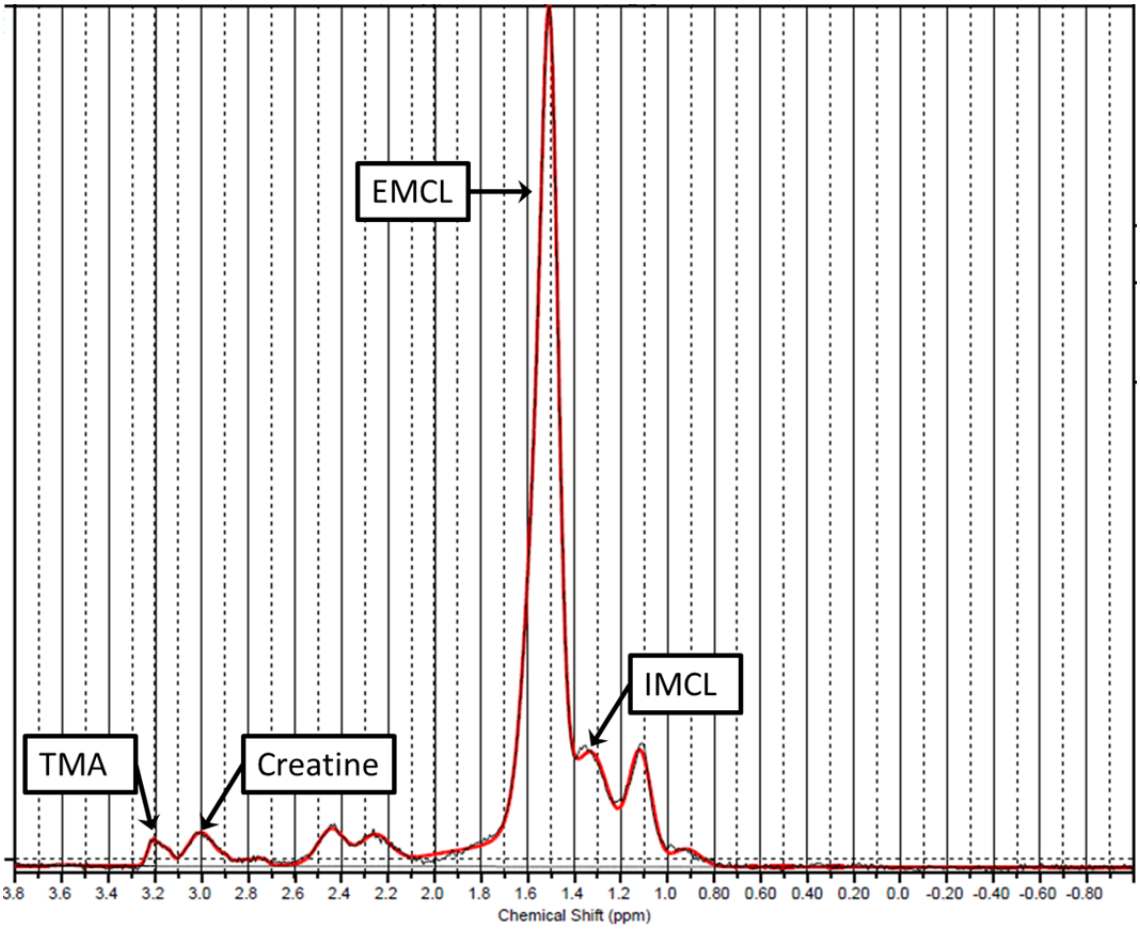

Figure 3: Histogram representing the distribution of log[TMA/Cr] ratios in controls (transparent bars) and participants with FSHD (blue bars).

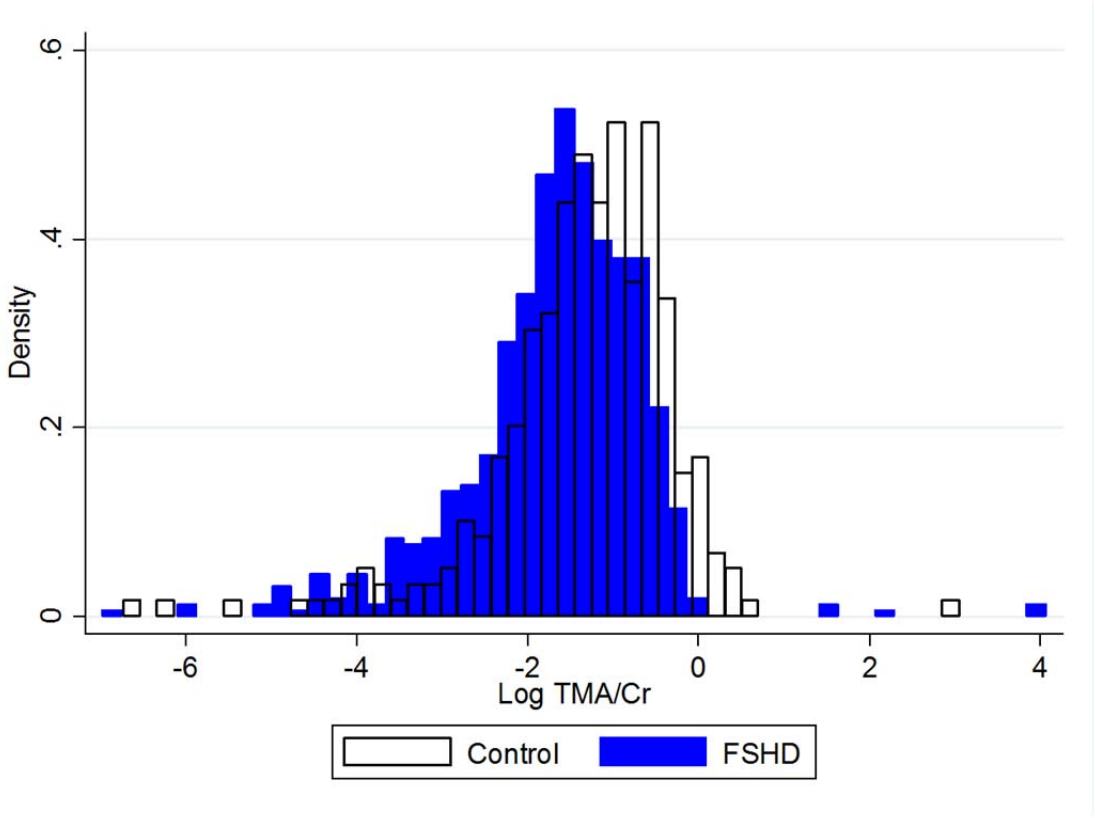

Figure 4: Histograms showing the distribution of additional metabolites analyzed from multivoxel muscle MRS. Transparent bars represent data from controls and blue bars represent data from participants with FSHD.

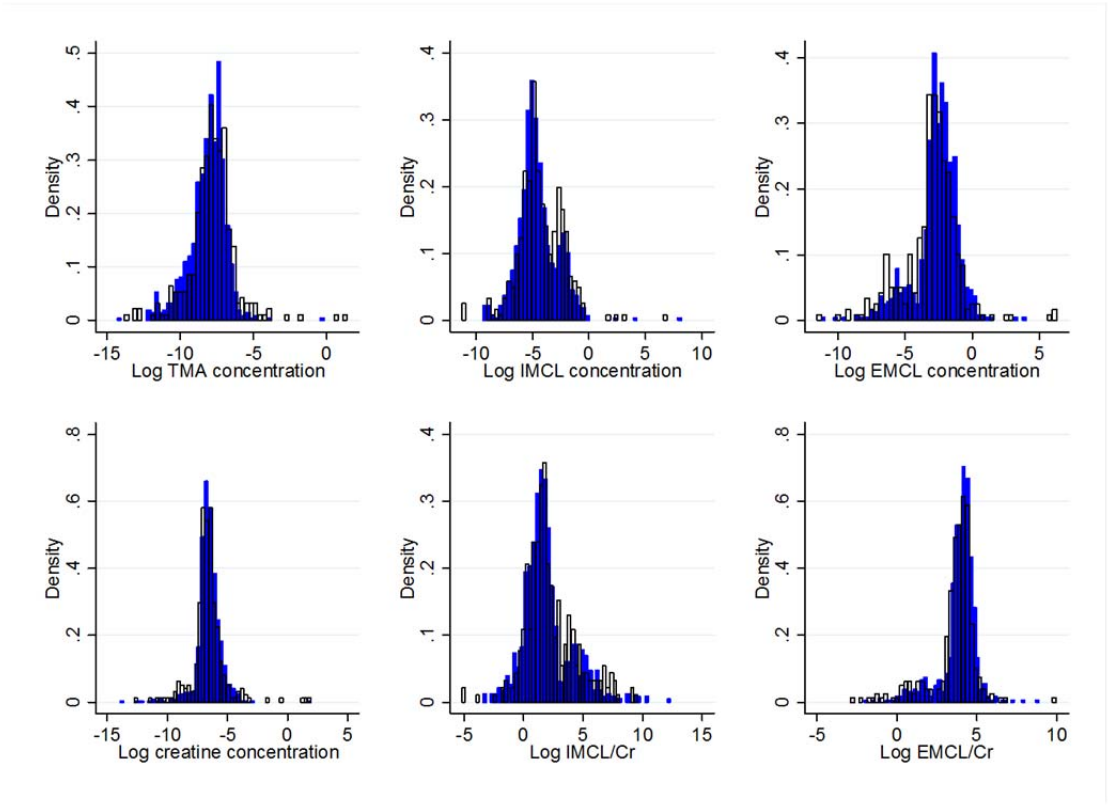

Figure 5: Fitted regression lines showing the association between hamstrings strength (left) and 10-meter walk time (right) and the mean log[TMA/Cr] ratio in hamstring muscles of participants with FSHD.

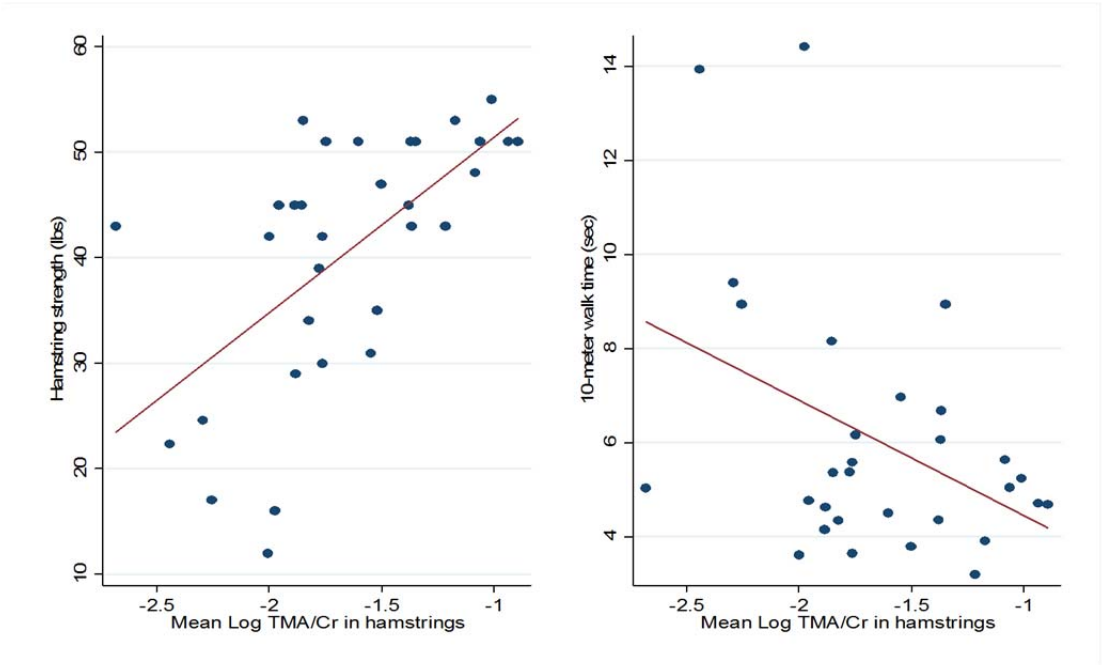

Figure 6: Box plots comparing metabolite concentration measured at baseline and after 18-24 months of follow-up in 10 participants with FSHD.

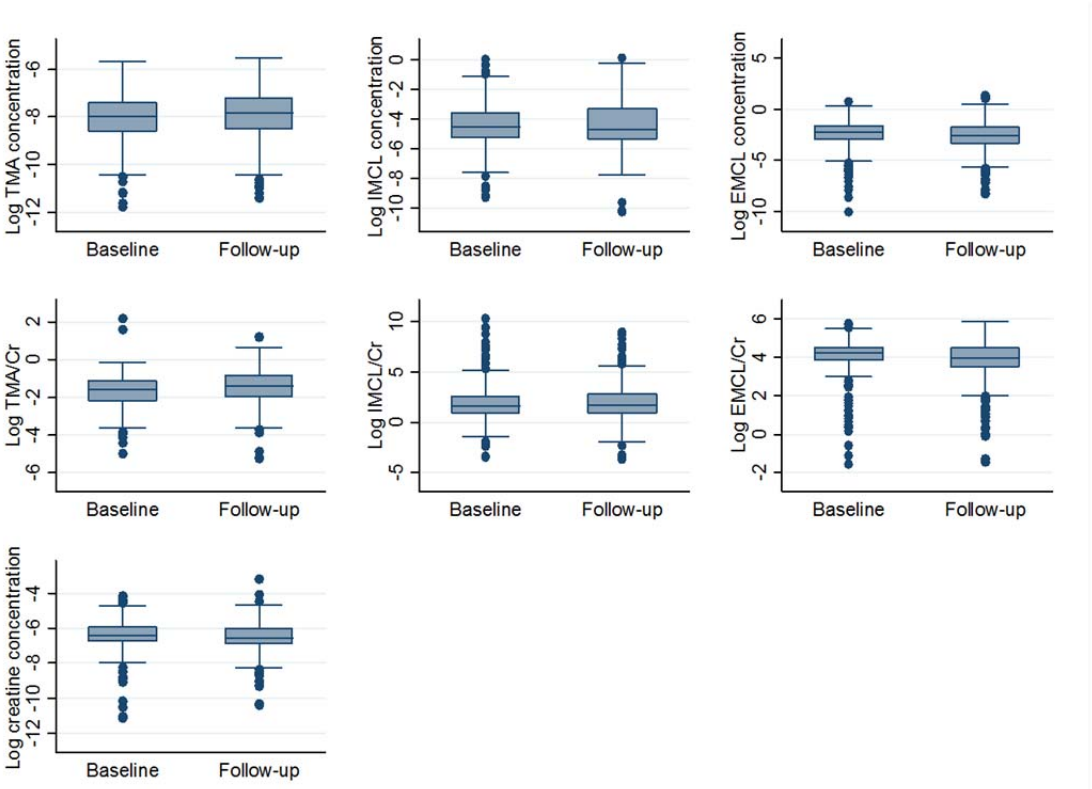

Figure 7: Bland-Altman plots showing the distribution of the differences in metabolite concentrations between baseline and follow-up scans. Each point represents an individual muscle within a single participant with FSHD.

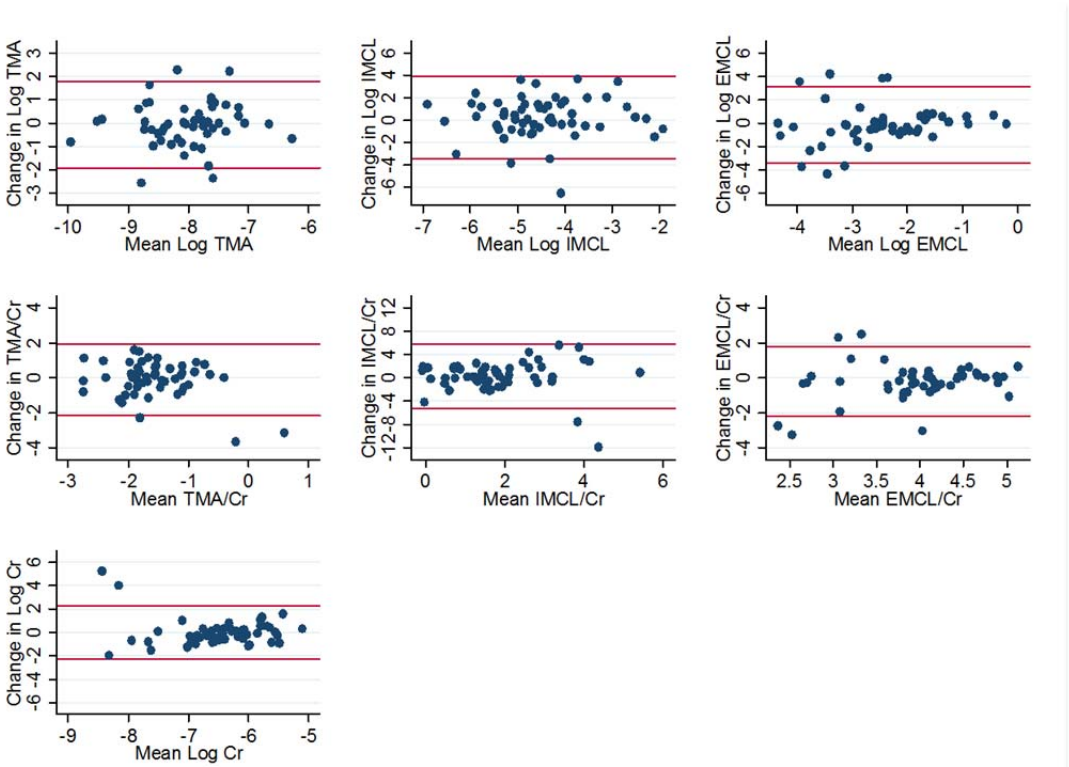

Conclusion

Few technological advances have changed the landscape of medical diagnostics as much as magnetic resonance imaging. MRI offers a wealth of both visual and quantitative data on the pathological and molecular characteristics of biological tissue, and its role in medicine continues to expand. Our work seeks to take several important steps in the development of MRI in the study of hereditary muscle diseases. Whole-body MRI was used to obtain anatomic images of large regions of muscle and to uncover significant associations between radiographic and clinical measurements in adults with FSHD. We also used multivoxel magnetic resonance spectroscopy to evaluate lower extremity muscles in people with FSHD and controls. We were able to show that metabolite concentrations can differ between affected and unaffected participants, even in muscles that appear normal on anatomic imaging. We further determined that metabolite concentrations obtained via magnetic resonance spectroscopy were significantly associated with muscle strength.

As we move forward in developing imaging protocols for use in clinical trials, researchers face several important challenges. One of these challenges is the transition from the primarily qualitative evaluation of radiographic data that predominates in clinical radiology to quantitative measurements that can enhance research studies. Researchers will also need to establish standardized protocols that ensure that the acquisition, processing, and analysis of images at different centers are comparable. Another challenge will be characterizing changes in radiographic measurements that occur as disease progresses over time. This is particularly relevant for MRI, which can often identify pathology before it is clinically detectable. Understanding the relationships between clinical and imaging observations will be crucial to the accurate interpretation of imaging biomarkers in clinical trials. Researchers also face the challenge of developing methods of combining different types of data obtained through MRI. One of the major

advantages of MRI is the ability to examine tissue using multiple sequences, and multiparametric outcome measurements that consolidate data from these sequences could improve their ability to detect and monitor disease pathology.

Although extensive work needs to be done to optimize and validate imaging biomarkers, magnetic resonance imaging offers a valuable potential solution to the paucity of biomarkers and surrogate outcome measures in muscular dystrophy research. Overcoming this obstacle will take a major step forward in establishing clinical trial readiness in these severely debilitating diseases.

CURRICULUM VITAE FOR ACADEMIC PROMOTION
The Johns Hopkins University School of Medicine

Doris G. Leung, MD **October,** **2016**

DEMOGRAPHIC AND PERSONAL INFORMATION

Current Appointments

2015-present Assistant Professor, Department of Neurology, The Johns Hopkins University School of Medicine, Kennedy Krieger Institute Center for Genetic Muscle Disorders

Personal Data

Center for Genetic Muscle Disorders
Kennedy Krieger Institute
716 N. Broadway, Room 411
Baltimore, MD 21205
Telephone: (443) 923-9521
Fax: (443) 923-9515
leungd@kennedykrieger.org

Education and Training

Undergraduate

1997-2001 B.A., Biochemical Sciences (magna cum laude), Harvard College, Cambridge, MA

Doctoral/Graduate

2001-05 M.D., Duke University School of Medicine, Durham, NC
2013-2016 Ph.D. Candidate, The Johns Hopkins Bloomberg School of Public Health, Graduate Training Program in Clinical Investigation, Baltimore, MD

Post-doctoral

2005-06 Intern, Internal Medicine, Duke University Medical Center, Durham, NC
2006-09 Resident, Neurology, Stanford University Medical Center, Stanford, CA
2009-10 Fellow, Clinical Neurophysiology, Stanford University Medical Center, California Pacific Medical Center, Stanford, CA
2010-11 Certificate, Science of Clinical Investigation, The Johns Hopkins Bloomberg School of Public Health, Baltimore, MD
2010-14 Translational Research Fellowship in Muscular Dystrophy, Center for Genetic Muscle Disorders, The Kennedy Krieger Institute, Baltimore, MD

Professional Experience

2011-2014 Contract Physician, Department of Neurology - EMG Clinic, The Johns Hopkins Bayview Medical Center, Baltimore, MD
2014-2015 Instructor, Department of Neurology, The Johns Hopkins University School of Medicine, The Kennedy Krieger Institute Center for Genetic Muscle Disorders, Baltimore, MD

2015-present Assistant Professor, Department of Neurology, The Johns Hopkins University School of Medicine, The Kennedy Krieger Institute Center for Genetic Muscle Disorders, Baltimore, MD

RESEARCH ACTIVITIES

Peer Reviewed Original Science Publications

1. Farzan M, Schnitzler CE, Vasilieva N, **Leung D,** and Choe H. "BACE2, a B-secretase homolog, cleaves at the *B* site and within the amyloid-B region of the amyloid-B precursor protein." *Proc Natl Acad Sci.* 2000 Aug; 97(17): 9712-9717.
2. Farzan M, Schnitzler C, Vasilieva N, **Leung D,** Kuhn J, Gerard C, Gerard NP, and Choe H. "Sulfated Tyrosines Contribute to the Formation of the C5a Docking Site of the Human C5a Anaphylatoxin Receptor." *J Exp Med.* 2001 May; 193(9): 1059-1065.
3. Pittman AM, Myers AJ, Abou-Sleiman P, Fung HC, Kaleem M, Marlowe L, Duckworth J, **Leung D,** Williams D, Kilford L, Thomas N, Morris CM, Dickson D, Wood NW, Hardy J, Lees AJ, de Silva R. "Linkage disequilibrium fine mapping and haplotype association analysis of the tau gene in progressive supranuclear palsy and corticobasal degeneration." *J Med Genet.* 2005 Nov; 42(11):837-46. Epub 2005 Mar 25.
4. Myers AJ, Kaleem M, Marlowe L, Pitt man AM, Lees AJ, Fung HC, Duckworth J, **Leung D,** Gibson A, Morris CM, de Silva R, Hardy J. "The Hl c haplotype at the MAPT locus is associated with Alzheimer's disease." *Hum Mol Genet.* 2005 Aug 15; 1 4(16):2399-404. Epub 2005 Jul 6.
5. Myers AJ, Pittman AM, Zhao AS, Rohrer K, Kaleem M, Marlowe L, Lees A, **Leung D,** McKeith IG, Perry RH, Morris CM, Trojanowski JQ, Clark C, Karlawish J, Arnold S, Forman MS, Van Deerlin V, de Silva R, Hardy J. "The MAPT Hlc risk haplotype is associated with increased expression of tau and especially of 4 repeat containing transcripts." *Neurobiol Dis.* 2007 Mar; 25(3):561-70. Epub 2006 Dec 15.
6. Coon KD, Myers AJ, Craig DW, Webster JA, Pearson JV, Lince DH, Zismann VL, Beach TG, **Leung D,** Bryden L, Halperin RF, Marlowe L, Kaleem M, Walker DG, Ravid R, Heward CB, Rogers J, Papassotiropoulos A, Reiman EM, Hardy J, Stephan DA. "A high-density whole-genome association study reveals that APOE is the major susceptibility gene for sporadic late-onset Alzheimer's disease." *J Clin Psychiatry.* 2007 Apr; 68(4):613-8.
7. Reiman EM, Webster JA, Myers AJ, Hardy J, Dunckley T, Zismann VL, Joshipura KD, Pearson JV, Hu-Lince D, Huentelman MJ, Craig DW, Coon KD, Liang WS, Herbert RH, Beach T, Rohrer KC, Zhao AS, **Leung D,** Bryden L, Marlowe L, Kaleem M, Mastroeni D, Grover A, Heward CB, Ravid R, Rogers J, Hutton ML, Melquist S, Petersen RC, Alexander GE, Caselli RJ, Kukull W, Papassotiropoulos A, Stephan DA. "GAB2 alleles modify Alzheimer's risk in APOE epsilon4 carriers." *Neuron.* 2007 Jun 7; 54(5):713-20.
8. Webster JA, Myers AJ, Pearson *N ,* Craig DW, Hu-Lince D, Coon KD, Zismann VL, Beach T, **Leung D,** Bryden L, Halperin RF, Marlowe L, Kaleem M, Huentelman MJ, Joshipura K, Walker D, Heward CB, Ravid R, Rogers J, Papassotiropoulos A, Hardy J, Reiman EM, Stephan DA. "Sorll as an Alzheimer's Disease Predisposition Gene?" *Neurodegener Dis.* 2008; 5(2):60-4. Epub 2007 Nov 1.
9. Myers AJ, Gibbs JR, Webster JA, Rohrer K, Zhao A, Marlowe L, Kaleem M, **Leung D,** Bryden L, Nath P, Zismann VL, Joshipura K, Huentelman MJ, Hu-Lince D, Coon KD, Craig DW, Pearson *N ,* Holmans P, Heweard CB, Reiman EM, Stephan D, Hardy J. "A survey of genetic human cortical gene expression." *Nature Genetics.* 2007 Dec; 39(12):1494-9. Epub 2007 Nov 4.

10. Webster JA, Gibbs JR, Clarke J, Ray M, Zhang W, Holmans P, Rohrer K, Zhao A, Marlowe L, Kaleem M, McCorquodale DS 3rd, Cuello C, **Leung D,** Bryden L, Nath P, Zismann VL, Joshipura K, Huentelman MJ, Hu Lince D, Coon KD, Craig DW, Pearson JV; NACC-Neuropathology Group, Heward CB, Reiman EM, Stephan D, Hardy J, Myers AJ. "Genetic control of human brain transcript expression in Alzheimer disease." *Am J Hum Genet.* 2009 Apr; 84(4):445-58.
11. Webster, J, Reiman EM, Zismann VL, Joshipura KD, Pearson *N ,* Hu-Lince D, Huentelman MF, Craig DW, Coon KD, Beach T, Rohrer KC, Zhao AS, **Leung D,** Bryden L, Marlowe L, Kaleem M, Mastroeni D, Grover A, Rogers J, Heun R, Jessen F, Kolsch, H, Heward CB, Ravid R, Hutton ML, Milquist S, Petersen RC, Caselli, RJ, Papassotiropoulos A, Stephan DA, Hardy J, Myers A. "Whole genome association analysis shows that ACE is a risk factor for Alzheimer's disease and fails to replicate most candidates from meta-analysis." *Int J Mol Epidemiol Genet.* 2010; 1(1):19-30.
12. Rahimov F, King OD, **Leung DG,** Bibat GM, Emerson CP, Kunkel LM, Wagner KR. "Transcriptional profiling in facioscapulohumeral muscular dystrophy to identify candidate biomarkers." *Proc Natl Acad Sci.* 2012 Oct 2; 109(40): 16234-9
13. Faridian-Aragh N, Wagner KR, **Leung DG,** Carrino JA. "MRI Phenotyping of Becker Muscular Dystrophy." *Muscle and Nerve.* 2014 Dec; 50(6):962-7
14. **Leung DG,** Herzka DA, Thompson WR, He B, Bibat G, Tennekoon G, Russell SD, Schuleri KH, Lardo AC, Kass DA, Thompson RE, Judge DP, Wagner KR. "Sildenafil does not improve cardiomyopathy in Duchenne/Becker muscular dystrophy." *Ann Neurol.* 2014; 76(4)541-9.
15. **Leung DG,** Carrino JA, Wagner KR, Jacobs MA. "Whole-body MRI evaluation of facioscapulohumeral muscular dystrophy." *Muscle and Nerve*, 2015; 52(4):512-20.
16. Wong, EG, Parker AM, **Leung DG,** Brigham EP, Arbaje AI. "Association of Severity of Illness and Intensive Care Unit Readmission: A Systematic Review." *Heart & Lung: The Journal of Acute and Critical Care*, 2016 Jan-Feb; 45(1):3-9.e2.

Inventions, Patents, Copyrights
Not applicable

Extramural Sponsorship

Current Grants

2015-2020 Magnetic resonance imaging and spectroscopy biomarkers for facioscapulohumeral muscular dystrophy
K23NS091379-01 Mentored Patient-Oriented Research Career Development Award National Institutes of Neurological Disorders and Stroke
$881,794
PI: Leung D, 85% effort

Previous

2010-2011 Muscle tissue collection and analysis of genetic biomarkers for FSHD Wellstone
Clinical Fellowship Grant
Biomedical Research Institute Senator Paul D. Wellstone Muscular Dystrophy Cooperative Research Center for FSHD Research
$50,000

PI: Wagner K
Role: Clinical Research Fellow, 100%

2011-2013 Magnetic Resonance Spectroscopy Imaging as a Biomarker for FSHD
Clinical Research Training Fellowship Grant
American Academy of Neurology
$130,000
PI: Leung D, 80%

2012-2014 Magnetic Resonance Imaging and Spectroscopy Biomarkers in FSHD
Irene Lai Research Grant
FSH Society
$98,390
PI: Wagner K
Role: Co-investigator, 0% effort

2014-2015 Whole-body MRI and MR spectroscopy as skeletal muscle biomarkers
KL2TR001077 Mentored Career Development Award
Johns Hopkins Clinical Research Scholars Program Grant
$58,650
PI: Leung D, 85% effort

Research Program Building/Leadership

IRB protocols – current

2010-present Facioscapulohumeral disease biomaterial of Wellstone Core
NA_ 00019985
Role: Sub-investigator

2011-present Magnetic Resonance and Spectroscopy Biomarkers for Facioscapulohumeral Muscular Dystrophy
NA_ 00065256
Role: Principal Investigator

2013-present Collection of Data from Muscle Strength Testing
NA_ 00082223
Role: Sub-investigator

2014-present A phase II randomized, double-blind, placebo-controlled, multiple ascending dose study to evaluate the safety, efficacy, pharmacokinetics and pharmacodynamics of PF-06252616 in ambulatory boys with Duchenne muscular dystrophy
IRB00049415
Role: Sub-investigator

2014-present An Open-label, Multi-center, 48-week study with concurrent untreated control arm to evaluate the efficacy and safety of Eteplirsen in Duchenne Muscular Dystrophy

IRB00040305
Role: Sub-investigator

2015-present An open-label, multi-center study to evaluate the safety and tolerability of eteplirsen in patients with advanced stage Duchenne muscular dystrophy
IRB00056437
Role: Sub-investigator

2015-present A randomized, double-blind, placebo-controlled, dose-titration, safety, tolerability, and pharmacokinetics study followed by an open-label safety and efficacy evaluation of SRP-4045 in advanced-stage patients with Duchenne muscular dystrophy amenable to exon 45 skipping
IRB00079233
Role: Sub-investigator

2015-2016 A Safety and Tolerability Study of Multiple Doses of ISIS-DMPKRx in Adults with Myotonic Dystrophy Type 1
IRB00052515
Role: Site Principal Investigator

2015-2016 An open-label, intrapatient dose escalation study to evaluate the safety, tolerability, immunogenicity, and biological activity of ATYR1940 in patients with limb girdle and facioscapulohumeral muscular dystrophies
IRB00074941
Role: Sub-investigator

2015-present A multi-site, randomized, placebo-controlled, double-blind, multiple ascending subcutaneous dose study to evaluate the safety, tolerability and pharmacokinetics of BMS-986089 in ambulatory boys with Duchenne muscular dystrophy
IRB00077885
Role: Sub-investigator

2016-present An open-label, expanded access program intended to provide treatment with MP-104 (deflazacort) to U.S. children, adolescents, and/or adults with Duchenne muscular dystrophy
IRB00097299
Role: Sub-investigator

2016-present A Phase 1b/2, Open-Label, Multiple Ascending Dose Study to Evaluate the Safety, Tolerability, Efficacy, Pharmacokinetics and Pharmacodynamics of PF-06252616 in Ambulatory Participants with LGMD2I
IRB00089732
Role: Sub-investigator

2016-present A Multicenter, Open-Label Extension Study to Evaluate the Long-term Safety of PF-06252616 in Boys with Duchenne Muscular Dystrophy
IRB00110715
Role: Sub-investigator

IRB protocols – past

2010-2013	Clinical Trial of Sildenafil in Dystrophin Deficiency NA_00036602 Role: Sub-investigator
2010-2013	An exploratory study to assess two doses of GSK2402968 in the treatment of ambulant boys with Duchenne muscular dystrophy NA_00051932 Role: Sub-investigator
2013-2015	Duchenne Muscular Dystrophy: Double-Blind Randomized Trial to Find the Optimum Steroid Regimen (FOR-DMD) NA_00077118 Role: Sub-investigator
2014-2015	Bone health in Facioscapulohumeral muscular dystrophy: A cross-sectional study IRB00031738 Role: Sub-investigator
2013-2016	A Phase lb Open-Label, Single and Multiple Ascending Dose Study to Evaluate the Safety, Tolerability and Pharmacokinetics of HT-100 in Patients with Duchenne Muscular Dystrophy (HALO DMD-01) NA_00082081 Role: Sub-investigator
2014-2016	An open-label extension study of HT-100 in patients with Duchenne Muscular Dystrophy who have completed protocol HALO-DMD-101 NA_00086591 Role: Sub-investigator
2014-2016	An open-label extension study of the long-term safety, tolerability and efficacy of drisapersen in US and Canadian subjects with Duchenne Muscular Dystrophy IRB00046817 Role: Sub-investigator
2015-2016	HT-100 long-term safety and pharmacodynamics in patient with DMD who have completed protocols HALO-DMD-01 and HALO-DMD-02 IRB00068303 Role: Sub-investigator
2015-2016	A feasibility study of outcome measures in adult LGMD2I IRB00074940 Role: Sub-investigator
2015-2016	An open-label extension study of the long-term safety, tolerability and efficacy of drisapersen in subjects with Duchenne Muscular Dystrophy IRB00079299

Role: Sub-investigator

EDUCATIONAL ACTIVITIES

Educational Publications

Peer-reviewed publications

1. **Leung DG,** Germain-Lee EL, Denger BE, and Wagner KR. "Report on the Second Endocrine Aspects of Duchenne Muscular Dystrophy Conference, December 1-2, 2010, Baltimore, Maryland, USA." *Neuromuscul Disord,* 2011; 21(8):594-601.

Invited Review Articles

1. **Leung DG,** Wagner KW. "Therapeutic Advances in Muscular Dystrophy." Invited Review. *Ann Neurology,* 2013 Sep; 74(3):404-11.

Case Reports

2. **Leung DG,** Taylor HA, Lindy AS, Basehore MJ, Mammen AL. "A case of progressive quadriceps weakness and hyperCKemia mimicking inclusion body myositis." *Arthritis Care and Research,* 2014; 66(2):328-333.

Book Chapters, Monographs

1. **Leung DG.** "Neuromuscular Diseases." In: Hayden Gephart, M, ed. *Tarascon Clinical Neurology Pocketbook*. Burlington, MA: Jones & Bartlett Learning, 71-78, 2013.
2. **Leung DG**. "Other Proven and Putative Autoimmune Disorders of the Peripheral Nervous System: Myasthenia Gravis." In: Johnston M, Adams H, and Fatemi SA, eds. *Neurobiology of disease,* 2nd ed. New York, NY: Oxford University Press, 714-18, 2016.
3. **Leung DG.** "Neuropathies Associated with Infection or Toxic Exposure." In: Johnston M, Adams H, and Fatemi SA, eds. *Neurobiology of disease,* 2nd ed. New York, NY: Oxford University Press, 815-30, 2016.

Teaching

Classroom Instruction

2013-2014	Neuropsychology Department Genetics/Congenital Disorders Clinic conference, "Overview of muscular dystrophy," The Kennedy Krieger Institute
2013	Pediatric Rehabilitation Department conference, "Myopathy," The Kennedy Krieger Institute
2014-present	Neurology Clerkship Lecture Series, "Numb and weak: An Introduction to Neuromuscular Disease," The Johns Hopkins University School of Medicine
2016	Physical Medicine and Rehabilitation Resident Lecture Series, "Genetic Muscle Disease," The Johns Hopkins University School of Medicine

Clinical Instruction

2011-present	PM&R Residents EMG Clinic, Attending physician, The Johns Hopkins Bayview Medical Center
2012-present	Neurology Clerkship EMG Clinic, Attending physician, The Johns Hopkins Bayview Medical Center
2013	Transition to the Wards for 2nd year medical students, Preceptor, The Johns Hopkins Hospital

2016 Clinical Skills Course for 1st year medical students, Preceptor, The Johns Hopkins Hospital

Educational Program Building / Leadership

2012-2015 Undergraduate Clinical Practicum in Muscular Dystrophy, Kennedy Krieger Institute Muscle Disorders Clinic, Preceptor

Educational Extramural Funding

Not applicable

CLINICAL ACTIVITIES

Certification

Medical, other state/government licensure

2005-2006 North Carolina, 127989
2006-2010 California, A98786
2010-present Maryland, D0071037

Boards, other specialty certification

2009 American Board of Psychiatry and Neurology, Neurology, #55752
2010 American Board of Psychiatry and Neurology, Clinical Neurophysiology, #2185

Clinical (Service) Responsibilities

2011-present EMG clinic, attending, ½ day per week, The Johns Hopkins Bayview Medical Center
2014-present Muscle Disorders Clinic, attending, ½ day twice monthly, The Kennedy Krieger Institute

Clinical Program Building / Leadership

Not applicable

Clinical Extramural Funding

Not applicable

SYSTEM INNOVATION AND QUALITY IMPROVEMENT ACTIVITIES

Not applicable

ORGANIZATIONAL ACTIVITIES

Institutional Administrative Appointments

Not applicable

Editorial Activities

Editorial Board appointments

Not applicable

Journal Reviewer

05/2014 *Arthritis Care and Research*
05/2014 *Annals of Neurology*
05/2015 *Neuromuscular Disorders*
10/2015 *Muscle and Nerve*

Advisory Committees, Review Groups/Study Sections
Not applicable

Professional Societies
2006-present Member, American Academy of Neurology
2010-present Member, American Association of Neuromuscular and Electrodiagnostic Medicine

Conference Organizer, Session Chair
Not applicable

Consultantships
Not applicable

RECOGNITION

Awards, Honors
2003 Clinical Research Training Fellowship, National Institutes of Health
2009 Neurology resident teaching award, Stanford Hospital and Clinics neurology residency
2010 American Academy of Neurology Foundation Clinical Research Training Fellowship
2013 KL2 Mentored Career Development Award, Johns Hopkins Clinical Research Scholars Program
2016 National Institutes of Health Clinical Loan Repayment Award – National Institute of Neurological Disorders and Stroke

Invited Talk, Panels
05/2011 Invited speaker, FSH Society, Mid-Atlantic Member Meeting, "Update on Research in FSHD," Baltimore, MD
10/2014 Invited speaker, Muscular Dystrophy Association Make a Muscle Conference, "FSHD/LGMD," Howard Community College, Columbia, MD
10/2015 Invited speaker, American Association of Neuromuscular and Electrodiagnostic Medicine Annual Meeting, "MRIs as biomarkers for myopathies," Honolulu, HI
01/2016 Invited Speaker, Interdisciplinary Clinical Genetic Conference, "MRI Biomarkers in Myopathy," Baltimore, MD
04/2016 Invited speaker/panelist, Professional Development and Careers Office, Institute for Clinical and Translational Research, Office of Faculty Development, "Writing Successful K Applications: Beyond the Basics," Johns Hopkins University, Baltimore, MD
05/2016 Invited speaker, FSH Society, Mid-Atlantic Member Meeting, "Resolaris in FSHD," Baltimore, MD